| Technical Note | 1965-63 |
| --- | --- |
| | C. M. Rader |
| | B. Gold |
| Digital Filter Design Techniques | |
| | 23 December 1965 |

# Lincoln Laboratory

MASSACHUSETTS INSTITUTE OF TECHNOLOGY

Lexington, Massachusetts

MASSACHUSETTS INSTITUTE OF TECHNOLOGY

LINCOLN LABORATORY

# DIGITAL FILTER DESIGN TECHNIQUES
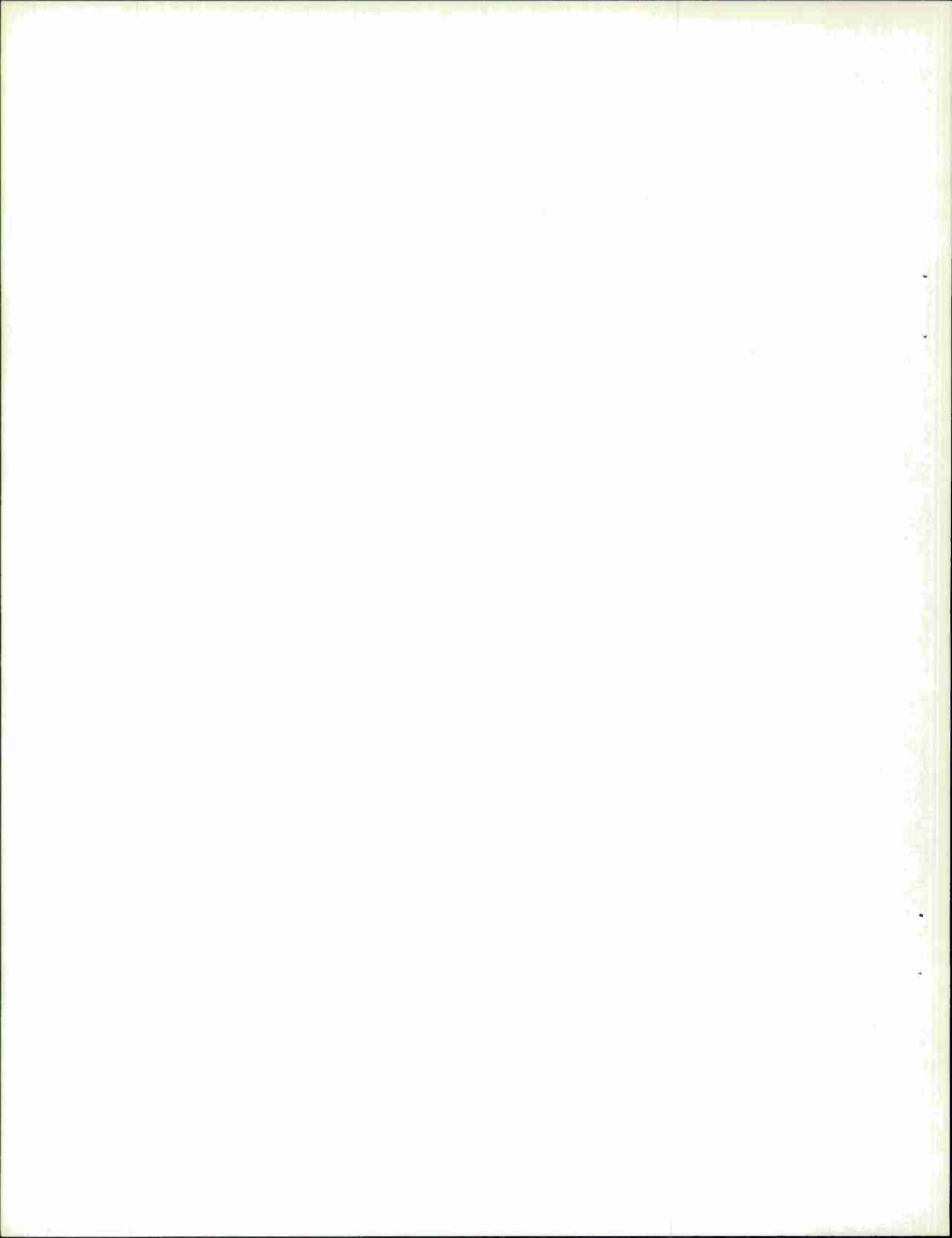
*C. M. RADER*

*B. GOLD*

*Group 62*

TECHNICAL NOTE 1965-63

23 DECEMBER 1965

LEXINGTON             MASSACHUSETTS

## ABSTRACT

Digital filtering is the process of spectrum shaping using digital components as the basic elements. Increasing speed and decreasing size and cost of digital components make it likely that digital filtering, already used extensively in the computer simulation of analog filters, will perform, in real-time devices, the functions which are now performed almost exclusively by analog components. In this paper, using the z-transform calculus, several digital filter design techniques are reviewed, and new ones are presented. One technique can be used to design a digital filter whose impulse response is like that of a given analog filter; another technique is suitable for the design of a digital filter meeting frequency response criteria. A third technique yields digital filters with linear phase, specified frequency response, and controlled impulse response duration. The effect of digital arithmetic on the behavior of digital filters is also considered.

iii
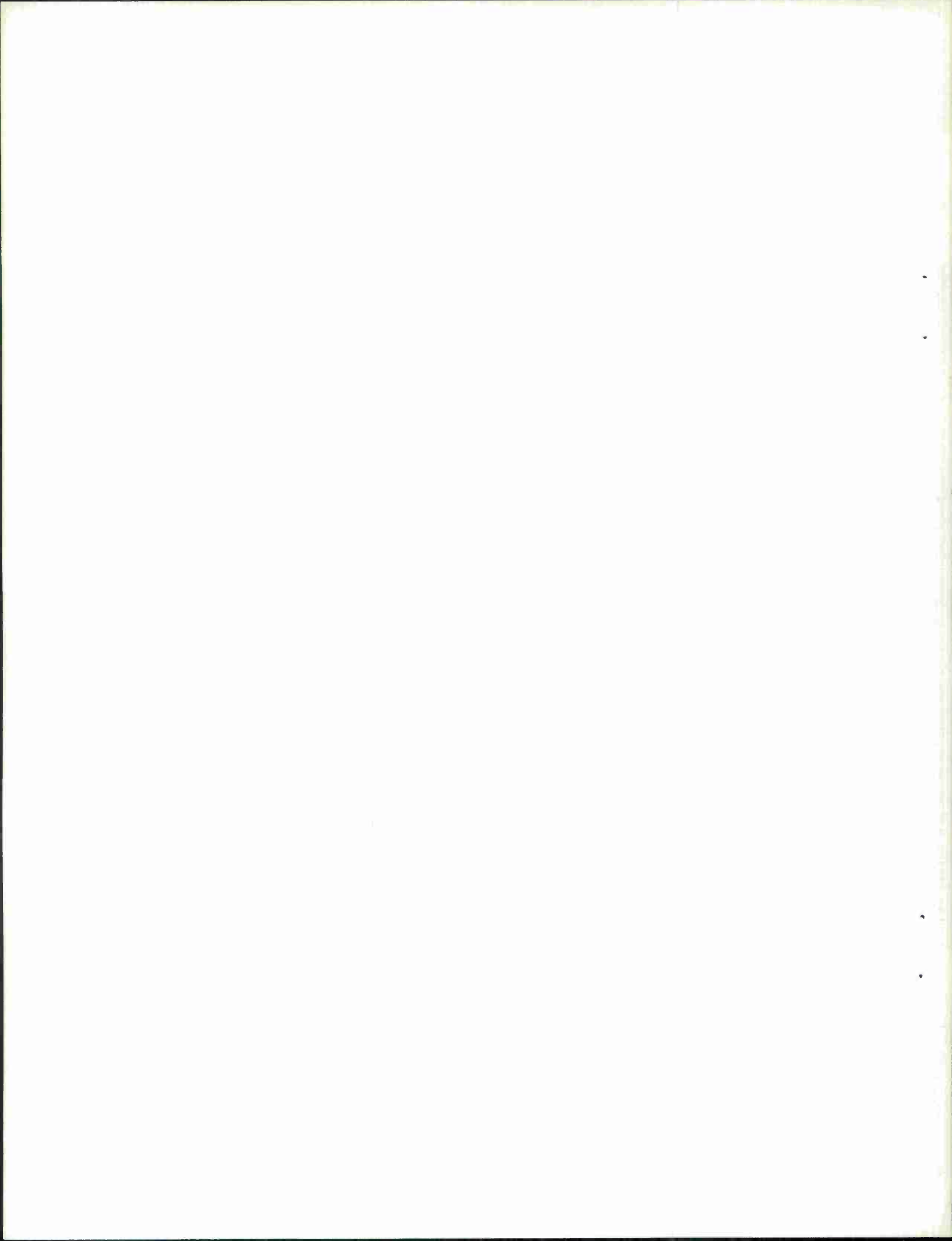
# DIGITAL FILTER   DESIGN TECHNIQUES

## SECTION 1

### a.   Introduction

Digital filtering is the process of spectrum shaping using digital hardware as the basic building block.   Thus the aims of digital filtering are the same as those of continuous filtering, but the physical realization is different.   Continuous filter theory is based on the mathematics of linear differential equations; digital filter theory is based on the mathematics of linear difference equations.

Interest in digital filtering derives from recent work on computer simulation of speech communications systems[1,2,3,4,5,6] and from problems arising in the processing of geophysical data[7].   In addition, however, increasing speeds and decreasing costs of microelectronic digital circuitry make possible the conception of real time digitized systems which perform the filtering operations presently performed exclusively by analog hardware.

The mathematical basis of digital filter theory is well known.   In addition to the mathematics literature on difference equations, a large body of work exists on the subject of sampled data systems and this work is of direct use in the design of digital filters.   Presently, no thorough treatment exists of digital filter design techniques and this paper is a start in that direction.   Emphasis will be placed on the frequency selectivity of filters rather than on the questions of stability and time response which are usually of interest in control systems.   However, it should be stressed that digital filters are mathematically equivalent to continuous systems with sampled data inputs and outputs.   In the continuous case, the sampling interval T usually depends on the nature of the discrete input, such as a pulsed radar return. The constraint on the sampling interval of a digital filter could also be caused by the computation time needed to execute the difference equations.

The basic mathematical tool of digital filters is the z transform calculus, used by Hurewicz[8] to develop his theory of pulsed filters.   We will first briefly review the z transform method and then present a number of design techniques with illustrative examples.

Real time digital filters should have several advantages over continuous filters.   They should adhere to the design so that no tuning would be required.   A greater variety of filters should be feasible, since no realizability problems (akin

to negative elements) arise. No special components are needed to realize filters with time varying coefficients. Aggregates of digital filters should be especially economic in the very low frequency band (.01 cycles per second to 1 cps), where the size of analog components becomes appreciable.

b.     Difference Equations of Digital Filters

An $m^{th}$ order linear difference equation may be written as:

$$y(nT) = \sum_{i=o}^{r} L_i\, x(nT-iT) - \sum_{i=1}^{m} K_i\, y(nT-iT) \tag{1}$$

The form of (1) emphasizes the iterative nature of the difference equation; given the m previous values of the output y and the $r + 1$ most recent values of the input x, the new output may be computed from (1). Physically, the input numbers are samples of a continuous waveform and real time digital filtering consists of performing the iteration (1) for each arrival of a new input sample. Design of the filter consists of finding the constants $K_i$ and $L_i$ to fulfill a given filtering requirement. Real time filtering implies that the execution time of the computer program for computing the right side of (1) be less than T, the sampling interval. Simulation programs in which the computations are not carried out in real time are understood to be simulations of the real time digital filters and the original sampling interval T of the continuous input data remains the reference parameter. It should be realized that quantization as well as sampling is performed on the continuous data before entry into the program and also, that the multiplications indicated in (1) contain an inherent round off error caused by finite register lengths, but for the most part these effects will be neglected. The effect of quantization is an important consideration and we will study it, to some extent, theoretically.

A useful pictorial representation of (1) consisting of unit delays (of time T), adders and multipliers is shown in Fig. 1.

Many practical designs utilize arrangements of simple (1st and 2nd order) difference equations. Arrangements can be serial, parallel or combinations of both. For example, the two equations:

$$\left.\begin{array}{l} y_1(nT) = K_{11}y_1(nT - T) + K_{12}y_1(nT - 2T) + L_{11}\, x(nT) \\[2em] y_2(nT) = K_{21}y_2(nT - T) + K_{22}y_2(nT - 2T) + L_{21}y_1(nT) \end{array}\right\} \tag{2}$$

2

constitute a serial arrangement whereby the output $y_1$ of the first equation is used as input to the second equation, as seen in Fig. 2. Similarly the equations:

$$y_1(nT) = K_{11}y_1(nT-T) + K_{12}y_1(nT-2T) + L_{11}\,x(nT)$$

$$y_2(nT) = K_{21}y_2(nT-T) + K_{22}y_2(nT-2T) + L_{21}\,x(nT) \tag{3}$$

$$y_3(nT) = y_1(nT) + y_2(nT)$$

shown in Fig. 3, constitute a parallel arrangement. The sets of equations (2) and (3) can be rewritten as single $4^{\text{th}}$ order difference equations; however, the significant properties of the digital filters are more readily understood via structures like Figs. 2 and 3.

Substantial literature[13] exists on the problems of pre-sampling filtering of the input and ultimate filtering of the output sequence to convert it to a continuous wave. We shall restrict ourselves to studying only the sequences.

c.    The Z Transform

In studying physical systems it is convenient to assume that the input begins at zero time and has magnitude zero beforehand. Thus $x(nT) = 0$ for $n < 0$ and therefore, in an inertial system such as that of equations (1), (2) or (3), $y(nT) = 0$ for $n < 0$.

The z transform of a sequence $x(nT)$ is defined as:

$$X(z) = \sum_{n=0}^{\infty} x(nT)\, z^{-n} \tag{4}$$

For many sequences, the infinite sum of (4) can be expressed in closed form. For example, the z transform of the sequence $x(nT) = 0$ for $n < 0$, $x(nT) = 1$ for $n \geq 0$ is $X(z) = \sum_{n=0}^{\infty} z^{-n} = \dfrac{1}{1-z^{-1}}$.

The transformation variable z is, in general, a complex variable and $X(z)$ is a function of a complex variable.

The z transform of a convergent sequence uniquely defines that sequence. By multiplying both sides of equation (4) by $z^{n-1}$ and integrating around any closed curve in the z plane which encloses all the singular points (poles) of $X(z)$ and the origin, we obtain:

$$x(nT) = \frac{1}{2\pi j} \oint X(z) z^{n-1} dz \tag{5}$$

where $j = \sqrt{-1}$ .

The inverse z transform (5) explicitly determines the sequence $x(nT)$ associated with a given $X(z)$. For sequences which converge to zero the unit circle can be the closed curve of integration.

d.   Solution of Difference Equations by z Transform Techniques

The z transform will now be used to obtain an explicit solution of the $m^{th}$ order linear difference equation (1). First, rewrite (1) as:

$$\sum_{i=0}^{m} K_i \, y(nT - iT) = \sum_{i=0}^{r} L_i \, x(nT - iT) \tag{6}$$

where $K_0 = 1$ .

Next, take the z transform of (6), to obtain:

$$\sum_{i=0}^{m} K_i \sum_{n=0}^{\infty} y(nT - iT) \, z^{-n} = \sum_{i=0}^{r} L_i \sum_{n=0}^{\infty} x(nT - iT) \, z^{-n} \tag{7}$$

Recognizing that the z transform of a sequence delayed by i samples is equal to the z transform of the original sequence multiplied by $z^{-i}$, equation (7) reduces to:

$$
\left.
\begin{array}{c}
Y(z) \sum\limits_{i=0}^{m} K_i \, z^{-i} = X(z) \sum\limits_{i=0}^{r} L_i \, z^{-i} \\[2em]
\text{or} \\[1em]
Y(z) = X(z) \dfrac{\sum\limits_{i=0}^{r} L_i \, z^{-1}}{\sum\limits_{i=0}^{m} K_i \, z^{-i}} = X(z) \, H(z)
\end{array}
\right\} \tag{8}
$$

4

Thus $Y(z)$ is explicitly determined as the product of the input $z$ transform and a system function $H(z)$ which is a rational fraction in $z^{-1}$ and is a function of the constant coefficients in the original difference equation. By the inverse $z$ transform (5), the output $y(nT)$ may be written as the inverse transform of $Y(z)$.

If we choose as the input sequence $x(nT) = \begin{cases} 1 \\ 0 \end{cases}$ for $\begin{matrix} n=0 \\ n \neq 0 \end{matrix}$, then in Eq. (8) $X(z) = 1$. Clearly the response to this input is the inverse $z$ transform of $H(z)$. Thus the sequence $1, 0, 0, \ldots \ldots$ plays the part in digital filter theory which the unit impulse plays in continuous filter theory. We shall refer to the inverse $z$ transform of $H(z)$ as the impulse response of a digital filter.

We can use Eq. (8) to derive a general representation of a digital filter which differs from that of Fig. 1. We can define an intermediate variable $W(z)$ corresponding to an intermediate sequence $w(nT)$, such that

$$W(z) = X(z) \frac{1}{\sum\limits_{i=0}^{m} K_i z^{-i}}$$

$$Y(z) = W(z) \sum\limits_{i=0}^{r} L_i z^{-i} \tag{8a}$$

The equations of (8a) result in simultaneous difference equations

$$w(nT) = x(nT) - \sum\limits_{i=1}^{m} K_i w(nT - iT)$$

$$y(nT) = \sum\limits_{i=0}^{r} L_i w(nT - iT) \tag{8b}$$

which lead to the structure shown in Fig. 4. This structure requires fewer delays (less storage) and may, therefore, be preferred for some realizations.

The primary importance of the system function $H(z)$ for our purposes is in its interpretation as a frequency selective function. Let us assume that the input is a sampled complex exponential wave.

$$x(nT) = e^{jn\omega T} \tag{9}$$

5

The solution to (6) for the input (9) is also a complex exponential wave which can be represented as:

$$y(nT) = F(e^{j\omega T}) e^{jn\omega T}$$ (10)

and, by substitution of (9) and (10) into (6) we quickly arrive at the result:

$$F(e^{j\omega T}) = \frac{\sum_{i=o}^{r} L_i e^{-ji\omega T}}{\sum_{i=o}^{m} K_i e^{-ji\omega T}} = H(e^{j\omega T})$$ (11)

The response to a sampled sinusoidal input can be readily found from (11).

e. Representation and Geometric Interpretation of System Function

We see that the system function $H(z)$ of (8) is interpretable as a frequency response function for values of $z$ on the unit circle in the complex $z$ plane. Note that the radian frequency $\omega$ is a continuous frequency so that the physical significance of the frequency response function is the same as that for continuous systems. Furthermore, the system function is a rational fraction whose numerator and denominator can be factored, so that $H(z)$ is uniquely defined, except for a constant multiplier, by the positions of its poles and zeros in the $z$ plane, and its value for any point $z$ determined directly by the distances of that point from the singularities. We are thus led directly to the geometric interpretation of Fig. 5 whereby the value of the frequency response function for any frequency $\omega$ is obtained by rotating by an angle $\omega T$ about the circle, measuring the distances to the zeros $R_1$, $R_2$ ...., the distances to the poles $P_1$, $P_2$ .... and then forming the ratio, so that in the example of Fig. 5,

$$|H(e^{j\omega T})| = \frac{R_1 R_2}{P_1 P_2 P_3}$$ (12)

$H(e^{j\omega T})$ also has associated with it a phase, which is given by:

$$\phi = \phi_1 + \phi_2 - (\psi_1 + \psi_2 + \psi_3)$$ (13)

The geometric basis for digital filter design is thus identical in principle with the geometric basis for continuous filter design with the following single and important difference: in the continuous filter, frequency is measured along the

6

imaginary axis in the complex s plane whereas in the digital filter, frequency is measured along the circumference of the unit circle in the z plane.

f.    Several Examples

### 1st order difference equation

The difference equation:

$$y(nT) = Ky(nT - T) + x(nT) \tag{14}$$

has the system function

$$H(z) = \frac{1}{1 - Kz^{-1}} \tag{15}$$

The frequency response function is then obtained by letting $z = e^{j\omega T}$ in (15), which yields,

$$|H(e^{j\omega T})| = \frac{1}{\sqrt{1 + K^2 - 2K \cos \omega T}} \tag{16}$$

$$\text{and } \phi = \text{angle of } H(e^{j\omega T}) = -\tan^{-1} \frac{\sin \omega T}{\cos \omega T - K}$$

### 2nd order difference equation

The difference equation:

$$y(nT) = K_1 y(nT - T) + K_2 y(nT - 2T) + x(nT) \tag{17}$$

has the system function

$$H(z) = \frac{1}{1 - K_1 z^{-1} - K_2 z^{-2}} \tag{18}$$

and the resulting frequency response magnitude

$$|H(e^{j\omega T})| = \frac{1}{\left[(1 - K_1 \cos \omega T - K_2 \cos 2\omega T)^2 + (K_1 \sin \omega T + K_2 \sin 2\omega T)^2\right]^{1/2}} \tag{19}$$

and phase

$$\phi(e^{j\omega T}) = -\tan^{-1} \frac{K_1 \sin \omega T + K_2 \sin 2\omega T}{1 - K_1 \cos \omega T - K_2 \cos 2\omega T} \tag{20}$$

The pole positions $\gamma$ and $\beta$ of H(z) are given by:

$$\left.\begin{array}{l} \gamma = \dfrac{K_1}{2} + \sqrt{\dfrac{K_1^2}{4} + K_2} \\[3em] \beta = \dfrac{K_1}{2} - \sqrt{\dfrac{K_1^2}{4} + K_2} \end{array}\right\} \tag{21}$$

For $K_2$ negative and $|K_2| > \dfrac{K_1^2}{4}$ the poles become complex conjugate and as they approach the unit circle, the well known resonance effect is evidenced. Figure 6 is a plot of magnitude vs. $\omega T$ for $T = 10^{-4}$, a resonant frequency of 1500 cps and several values of damping. In the vicinity of the poles, the magnitude function behaves very much like a continuous resonator. Of course, the magnitude and phase must be periodic in $\omega T$; this follows from the original premise of a sampled input and is embodied in the unit circle z plane representation. We state, without proof, the well known facts that all poles of H(z) must lie within the unit circle for stability and that poles and zeros must occur on the real axis or in conjugate complex pairs. Also, it should be clear from equation (8) that an mth order difference equation has a z transform system function containing m poles and r zeros, r being the number of unit delays of the input.

## SECTION 2

a. <u>General Discussion of Digital Filter Design Techniques</u>

Since much information is available on continuous filter design, a useful approach to digital filter design involves finding a set of difference equations having a system function H(z) which significantly resembles known analog system functions. The work of Hurewicz[8] provides a technique for doing this in an 'impulse invariant' way. By this we mean that the discrete responses to an impulse function (see section 1d) of the derived digital filter will be the samples of the continuous impulse response of the given continuous filter.

Digital filters can be specified from a desired squared magnitude function using procedures akin to that of Butterworth and Chebyshev continuous filter design procedure. This method will be described and realizability conditions discussed in an Appendix.

Another technique used by various workers[9, 10, 11, 12] uses conformal mapping to transform a known continuous filter function into a digital filter. We will refer to this technique as 'frequency invariant', since critical points on the continuous filter's magnitude vs frequency curve can be invariantly transformed into the z plane.

Finally, a technique referred to as 'frequency sampling', makes use of the special properties of an elemental digital filter. This elemental filter's frequency response curve resembles a $\frac{\sin x}{x}$ function and has a linear phase vs frequency characteristic. By suitably combining these elemental filters, a simple design technique for a large variety of digital filters can be developed.

Where the same filtering requirements can be adequately met by several different digital filters, the choice between them depends on the speed of execution of a computer program which performs the difference equation. An important factor in this speed is the number of multiplications (not counting multiplications by such factors as $\pm 1$ or $2^n$, which computers can do quickly). Some digital filters are able to meet essentially the same requirements as others with substantially fewer multiplications per output sample, and these are to be preferred. It is important to stress that speed of execution is the main limiting factor in the utilization of digital filtering methods.

9

b.    Technique  1 - Impulse Invariance

We first show that a digital filter with an impulse response equal to the sampled impulse response of a given continuous filter can be derived via the correspondence

$$Y(s) = \sum_{i=1}^{m} \frac{A_i}{s + s_i} \Rightarrow \sum_{i=1}^{m} \frac{A_i}{1 - e^{-s_i T} z^{-1}} = H(z) \tag{22}$$

The impulse response  k(t)  of a continuous filter is defined as the inverse Laplace Transform of its system function  Y(s), given in general form* by the left side of (22).  Similarly, the impulse response  h(nT)  of a digital filter is defined as the inverse  z  transform of its system function  H(z),  which can be expressed generally by the right side of (22).

Thus

$$k(t) = L^{-1}\left(\sum_{i=1}^{m} \frac{A_i}{s + s_i}\right) = \sum_{i=1}^{m} A_i e^{-s_i t} \tag{23}$$

If we desire that  $h(nT) = k(t)$,  $t = 0, T, 2T \ldots$ . \hfill (24)

$$h(nT) = \sum_{i=1}^{m} A_i e^{-s_i n T} \tag{25}$$

---

*To be completely general,  equation (22) should also include terms of the form

$$\frac{A_i}{(s + s_i)^{\ell}}$$

which correspond to terms of the form

$$\left[\frac{(-1)^{\ell-1}}{(\ell - 1)!} \frac{\partial^{\ell-1}}{\partial a^{\ell-1}} \left(\frac{A_i}{1 - e^{-aT} z^{-1}}\right)\right]\Bigg|_{a = s_i}$$

10

Taking the $z$ transform of (25)

$$H(z) = \sum_{n=o}^{\infty} h(nT) z^{-n} = \sum_{i=1}^{m} A_i \sum_{n=o}^{\infty} e^{-s_i nT} z^{-n} = \sum_{i=1}^{m} \frac{A_i}{1 - e^{-s_i T} z^{-1}} \qquad (26)$$

Thus the condition (24) that the impulse response of the digital filter be equal to the sampled impulse response of a given continuous filter $Y(s)$ leads to a digital filter defined by (26), where all constants $A_i$ and $s_i$ have already been specified from $Y(s)$. Thus, by means of the correspondence (22) $z$ transforms can be tabulated[13].

Example:

The simple one pole RC low pass filter is transformed to a digital filter via the correspondence:

$$\frac{a}{s+a} \;\rightarrow\; \frac{a}{1 - e^{-aT} z^{-1}} \qquad (27)$$

System functions of various resonant circuits may be expanded by partial fractions, leading to the correspondences

$$\frac{s+a}{(s+a)^2 + b^2} \;\rightarrow\; \frac{1 - e^{-aT} \cos b\, T\, z^{-1}}{1 - 2e^{-aT} \cos b\, T\, z^{-1} + e^{-2aT} z^{-2}} \qquad (28)$$

$$\frac{b}{(s+a)^2 + b^2} \;\rightarrow\; \frac{e^{-aT} \sin b\, T\, z^{-1}}{1 - 2e^{-aT} \cos b\, T\, z^{-1} + e^{-2aT} z^{-2}} \qquad (29)$$

c.  Design of a Digital Lerner Filter which is "Impulse Invariant"

The Lerner filter[14] is defined by the continuous system function

$$Y(s) = \sum_{i=1}^{m} \frac{B_i(s+a)}{(s+a)^2 + b_i^2} \qquad (30)$$

with $\qquad B_1 = \frac{1}{2}$ , $B_m = \frac{(-1)^{m+1}}{2}$ , $B_i = (-1)^{i+1}$ for $i = 2, \ldots, m-1$

11

and the pole positions $(-a + b_i)$ shown in Fig. 7. It has been shown that Lerner filters have a high degree of phase linearity and reasonably selective pass bands.

From the correspondence (28), the z transform of the digital Lerner filter is

$$H(z) = \sum_{i=1}^{m} \frac{B_i(1 - e^{-aT} \cos b_i T z^{-1})}{1 - 2e^{-aT} \cos b_i T z^{-1} + e^{-2aT} z^{-2}} \tag{31}$$

Figure 8 shows the digital realization of a 4th order band pass Lerner filter. Each of the four parallel sub outputs $y_i$ is computed by the difference equation

$$y_i(nT) = e^{-aT} \cos b_i T [2y_i(nT - T) - x(nT - T)] - e^{-2aT} y_i(nT - 2T) + x(nT) \tag{32}$$

$$i = 1, 2, 3, 4$$

and the output $y(nT)$ is given by:

$$y(nT) = \frac{1}{2} y_1(nT) - y_2(nT) + y_3(nT) - \frac{1}{2} y_4(nT) \tag{33}$$

d.     Gain of Digital Resonators

The correspondences (28) and (29) define two digital resonators which are 'impulse invariants' of given continuous resonators. In practice, digital resonators can be specified without reference to continuous resonators. Specification consists of placing the pair of complex conjugate poles and, in most cases, a single zero, from which the difference equation can be quickly derived. Since many digital filters are simple serial or parallel combinations of these resonators, it is important to understand their behavior.

The z transform of a resonator with poles at $z = r e^{\pm j\omega_r T}$ and a zero at q is

$$H(z) = \frac{1 - q z^{-1}}{1 - 2r \cos \omega_r T z^{-1} + r^2 z^{-2}} \tag{34}$$

The magnitude vs frequency function for (34) is $|H(e^{j\omega T})|$ and can be written down, by inspection, from Fig. 5, using the law of cosines.

12

$$|H(e^{j\omega T})| = \left[ \frac{1 + q^2 - 2q \cos \omega T}{[1 + r^2 - 2r \cos (\omega - \omega_r)T][1 + r^2 - 2r \cos (\omega + \omega_r)T]} \right]^{1/2} \quad (35)$$

Case 1  $q = \cos \omega_r T$

For values of $r$ close to unity, the value of $|H(e^{j\omega T})|$ at the resonance $\omega_r$ can be approximated by

$$|H(e^{j\omega T})| = \frac{1}{2(1 - r)\sqrt{r}} \quad (36)$$

which is independent of $\omega_r$. Thus, this choice of $q$ makes possible the design of an equal gain bank of resonators (or filters composed of these resonators) covering a wide frequency range.

For narrow band resonators in which $r$ is close to unity, (36) shows clearly that the gain at resonance is usually appreciably greater than unity. Knowledge of filter gains is required for determination of appropriate register word lengths.

Case 2  $q = r \cos \omega_r T$

For this case, the difference equation for (34) can be written

$$y(nT) = r \cos \omega_r T(2y(nT - T) - x(nT - T)) + r^2 y(nT - 2T) + x(nT) \quad (37)$$

Execution of (37) requires only 2 multiplication instructions compared to 3 multiplications for general $q$ and this case is thus of special interest for real time applications and when total computer running time is inordinately lengthy. Sensitivity of the resonant gain with the resonant frequency is greater than for Case 1.

Case 3  $q = 1$

This case yields zero gain at "d.c.", when $\omega_r = 0$, which is often desirable. As in Case 2, two multiplications are needed. The gain for $\omega_r T = \frac{\pi}{2}$ is $\sqrt{2}$ times the gain for $\omega_r T$ close to zero.

Case 4  $q = 0$

In this case, the zero disappears. In the design of formant vocoders, it is desirable to design resonators without zeros, but with constant gain for $\omega = 0$, independent of $\omega_r$. This is obtained from the digital system function:

13

$$H(z) = \frac{1 - 2r \cos \omega_r T + r^2}{1 - 2r \cos \omega_r Tz^{-1} + r^2 z^{-2}} \qquad (38)$$

e.   Design of Digital Filters from Continuous Filters Which Have Zeros at
     Infinity

A large class of analog filters are defined by system functions of the form

$$Y(s) = \frac{1}{\prod\limits_{i=1}^{m} (s + s_i)} \qquad (39)$$

where the denominator is a product.  Such filters have  m  poles at finite values of
s  and an  $m^{th}$  order zero for infinite  s.   Included in this category are Butterworth,
Chebyshev and Bessel filters.

In order to design impulse invariant digital filters based on  (39),  the pro-
cedure outlined in Section  2b  can be used;  $Y(s)$  is expanded in partial fractions,
the  $A_i$  are found and  $H(z)$  is obtained from the correspondence (22).  In general,
this causes zeros to appear in  $H(z)$,   although there were no finite zeros in  $Y(s)$.
However, when the poles at  $-s_i$  are close to the imaginary axis in the  s  plane, such
that  $e^{-s_i T}$  is close to unity,  the zeros of  $H(z)$  can be ignored and  $H(z)$  may be
approximated by

$$H(z) = \frac{1}{\prod\limits_{i=1}^{m} \left( 1 - e^{-s_i T} z^{-1} \right)} \qquad (40)$$

In fact, it can be shown that (39) and (40) correspond exactly if  $e^{-s_i T}$
can be replaced by  $1 - s_i T$.   In practice, digital band pass filters several hundred
cycles wide of the Bessel, Butterworth or Chebyshev type have been successfully
programmed for  10000  cycle sampling rates,  using the form (40).

Example  3 pole Butterworth Low Pass Filter

The system function of the continuous filter is

$$Y(s) = \frac{s_1 s_2 s_3}{(s + s_1)(s + s_2)(s + s_3)} \qquad (41)$$

14

with $\qquad s_1 = \omega_c, \; s_2 = \frac{1}{2}\left(1 + j\sqrt{3}\right)\omega_c, \; s_3 = \frac{1}{2}\left(1 - j\sqrt{3}\right)\omega_c$

$\omega_c$ being the cut-off frequency, defined by $|Y(j\omega_c)| = .707$. Expansion of (41) into partial fractions and the correspondence (22) leads to the $z$ transform

$$H(z) = \frac{\omega_c}{1 - e^{-\omega_c T}z^{-1}} + \frac{-\omega_c + e^{-\omega_c T/2}\left[\cos\frac{1}{2}\sqrt{3}\,\omega_c T + \frac{1}{\sqrt{3}}\sin\frac{1}{2}\sqrt{3}\,\omega_c T\right]\omega_c z^{-1}}{1 - 2e^{-\omega_c T/2}\cos\frac{1}{2}\sqrt{3}\,\omega_c T\, z^{-1} + e^{-\omega_c T}z^{-2}} \tag{42}$$

which has the diagrammatic representation shown in Fig. 9.

If a cascade representation is desired, (42) can be rewritten to give

$$H(z) = \frac{C z^{-1} + D z^{-2}}{\left(1 - e^{-\omega_c T}z^{-1}\right)\left(1 - 2e^{\frac{-\omega_c T}{2}}\cos\frac{\sqrt{3}}{2}\,\omega_c T z^{-1} + e^{-\omega_c T}z^{-2}\right)}$$

with $\quad C = \omega_c\left[e^{-\omega_c T} + e^{\frac{-\omega_c T}{2}}\left(\frac{1}{\sqrt{3}}\sin\frac{\sqrt{3}}{2}\,\omega_c T - \cos\frac{\sqrt{3}}{2}\,\omega_c T\right)\right]$

and $\quad D = \omega_c\left[e^{-\omega_c T} - e^{\frac{-3\omega_c T}{2}}\left(\frac{1}{\sqrt{3}}\sin\frac{\sqrt{3}}{2}\,\omega_c T + \cos\frac{\sqrt{3}}{2}\,\omega_c T\right)\right] \tag{43}$

$H(z)$ is seen to have two zeros, one at $z = 0$ and the other at $z = -\frac{D}{C}$. This zero is on the real axis and increases as $\omega_c T$ is increased from zero. Note that the denominator of (43) can be written down by inspection of the poles of the continuous filter, since an $s$ plane pole transforms directly into a $z$ plane pole via $z = e^{sT}$. Thus, the zero of (43) at $-\frac{D}{C}$ causes the only error in the assumption that an $s$ plane serial system transforms directly into a $z$ plane serial system.

For small $\frac{D}{C}$ the error is negligible, since the zero is nearly at the center of the $z$ plane unit circle and has no effect on the magnitude of $H(z)$. Figure 10 shows a plot of $\frac{D}{C}$ vs $\omega_c T$. We see, for example, that the zero moves about 5% to the right of the origin for $\omega_c T = .1$, which reduces the selectivity of the cascade approximation very slightly.

f.   Review of Butterworth and Chebyshev Filters

In this section, we review briefly design procedures for continuous Butterworth and Chebyshev filters, which will be needed in the later discussion of digital filter design.   More complete treatments are available in standard texts[15, 16, 17].

The Butterworth filter can be specified by the relationship.

$$|F(j\omega)|^2 = \frac{1}{1 + \left(\frac{\omega}{\omega_c}\right)^{2n}} \tag{44}$$

where $\omega_c$ is a cut-off frequency and $|F(j\omega)|^2$ is the squared magnitude of a filter transfer function.   The poles of equation (44) lie equally spaced on a circle of radius $\omega_c$ in the s plane, as shown in Fig. 11.   For n odd, there will be poles at angles of 0 and $\pi$; for n even, the first pole (beginning at angle 0) occurs at an angle of $\frac{\pi}{2n}$.   It can be shown that the desired transfer function F(s) is a rational function with unity numerator and denominator determined by the left half poles of Fig. 11.   Plots of $|F(j\omega)|$ of (44) for several values of n are shown in Fig. 12.   From these plots the selectivity properties of the Butterworth filter become clear.

The Chebyshev filter is specified by

$$|F(j\omega)|^2 = \frac{1}{1 + \epsilon^2 V_n^2\left(\frac{\omega}{\omega_c}\right)} \tag{45}$$

where $V_n(x)$ is a Chebyshev polynomial of order n which can be generated by the recursion formula

$$V_{n+1}(x) - 2x\, V_n(x) + V_{n-1}(x) = 0 \tag{46}$$

with          $V_1(x) = x$   and   $V_2(x) = 2x^2 - 1$

The Chebyshev polynomial has the property of equal ripple over a given range, which, with added specification of $\epsilon$, leads to a magnitude function of a form given by Fig. 13, an equal ripple in the pass band and a monotonic decay in the stop band.   The ripple amplitude $\delta$ is given by

16

$$\delta = 1 - \frac{1}{\sqrt{1 + \epsilon^2}} \tag{47}$$

The poles of equation (45) lie on an ellipse which can be determined totally by specifying $\epsilon$, $n$ and $\omega_c$. Figure 14 shows this ellipse, the vertical and horizontal apices being given by: $b\omega_c$, $a\omega_c$ where

$$b, a = \frac{1}{2} \left\{ \left( \sqrt{\epsilon^{-2} + 1} + \epsilon^{-1} \right)^{\frac{1}{n}} \pm \left( \sqrt{\epsilon^{-2} + 1} + \epsilon^{-1} \right)^{-\frac{1}{n}} \right\} \tag{48}$$

where the $b$ is given for the plus sign and $a$ for the minus sign. The poles on the ellipse may be geometrically related to the poles of two Butterworth circles of radius $a\omega_c$ and $b\omega_c$. The vertical position of the ellipse pole is equal to the vertical position of the pole on the small circle, while the horizontal position is that of the horizontal position of the large circle pole.

g.  Technique 2 - Digital Filter Specification From Squared Magnitude Function

We have seen in Section 2f that the Butterworth and Chebyshev filters are specified by choosing suitably selective squared magnitude functions such as in equations (44) and (45). The same procedure is possible for digital filters and is described in this section.

Having established in Section 1d that the digital filter system function $H(z)$ is a rational fraction in $z^{-1}$, it follows that $H(z)$ for $z$ on the unit circle is a rational fraction of $e^{j\omega T}$. Thus, the squared magnitude $|H(e^{j\omega T})|^2$ can always be expressed as the ratio of two trigonometric functions of $\omega T$.

An example of a squared magnitude function suitable for low pass filtering is

$$|H(e^{j\omega T})|^2 = \frac{1}{1 + \dfrac{\tan^{2n} \dfrac{\omega T}{2}}{\tan^{2n} \dfrac{\omega_c T}{2}}} \tag{49}$$

Equation (49) is plotted in Fig. 15 for $\omega_c T = \frac{\pi}{2}$ for several values of $n$. The curves obtained are similar to those of the Butterworth filter of equation (44) plotted in Fig. 11. The cut-off frequency $\omega_c$ plays the same role in both continuous and digital case.

Letting $z = e^{j\omega T}$, (49) may be rewritten

17

$$|H(z)|^2 = \frac{\tan^{2n} \dfrac{\omega_c T}{2}}{\tan^{2n} \dfrac{\omega_c T}{2} + (-1)^n \left(\dfrac{z-1}{z+1}\right)^{2n}} \tag{50}$$

We see that (50) is a rational fraction in $z$ which has a zero of order $2n$ at $z = -1$. The poles are found by substituting, in (50)

$$p = \frac{z-1}{z+1} \tag{51}$$

from which we can ascertain that the $2n$ poles of $p$ are uniformly spaced around a circle of radius $\tan \dfrac{\omega_c T}{2}$. The poles of $z$ are then readily found by the transformation inverse to (51), namely

$$z = \frac{1+p}{1-p} \tag{52}$$

Letting $p = x + jy$ and $z = u + jv$, we find from (52) the component relations

$$u(x, y) = \frac{1 - x^2 - y^2}{(1-x)^2 + y^2} \ ; \ v(x, y) = \frac{2y}{(1-x)^2 + y^2} \tag{53}$$

The circle containing the poles in the $p$ plane satisfies the equation

$$x^2 + y^2 = \tan^2 \frac{\omega_c T}{2} \tag{54}$$

From (53) and (54) it can be shown that the circle of (54) maps into a circle in the $z$ plane centered at $(u, v)$ with radius $\rho$

$$\left. \begin{aligned} u &= \frac{1 + \tan^2 \dfrac{\omega_c T}{2}}{1 - \tan^2 \dfrac{\omega_c T}{2}} = \sec \omega_c T \ , \quad v = 0 \\[2em] \rho &= \frac{2 \tan \dfrac{\omega_c T}{2}}{1 - \tan^2 \dfrac{\omega_c T}{2}} = \tan \omega_c T \end{aligned} \right\} \tag{55}$$

18

For odd values of $n$, the $2n$ poles of $p$ have the $x$ and $y$ coordinates

$$x_m = \tan \frac{\omega_c T}{2} \cos \frac{m\pi}{n}$$

$$m = 0, 1, \ldots 2n - 1 \qquad (56)$$

$$y_m = \tan \frac{\omega_c T}{2} \sin \frac{m\pi}{n}$$

For even values of $n$, the coordinates are

$$x_m = \tan \frac{\omega_c T}{2} \cos \frac{2m + 1}{2n} \pi$$

$$m = 0, 1, \ldots 2n - 1 \qquad (57)$$

$$y_m = \tan \frac{\omega_c T}{2} \sin \frac{2m + 1}{2n} \pi$$

From (53) and (56) the corresponding poles in the $z$ plane are computed to be

$$\left. \begin{array}{l} u_m = \dfrac{1 - \tan^2 \dfrac{\omega_c T}{2}}{1 - 2 \tan \dfrac{\omega_c T}{2} \cos \dfrac{m\pi}{n} + \tan^2 \dfrac{\omega_c T}{2}} \\[4em] v_m = \dfrac{2 \tan \dfrac{\omega_c T}{2} \sin \dfrac{m\pi}{n}}{1 - 2 \tan \dfrac{\omega_c T}{2} \cos \dfrac{m\pi}{n} + \tan^2 \dfrac{\omega_c T}{2}} \end{array} \right\} m = 0, 1 \ldots 2n - 1 \qquad (58)$$

Replacing $\dfrac{m\pi}{n}$ by $\dfrac{2m + 1}{2n} \pi$ yields equivalent formulas for $n$ even.

Example  Find the poles and zeros of the squared magnitude function of a low pass filter with 3 db attenuation at 1250 cps and with at least 20 db attenuation at 2000 cps. Let the sampling rate be 10000 cps.

The cut-off frequency of 1250 cps corresponds to $\omega_c T = 45^o$. The frequency 2000 cps corresponds to $\omega T = 72^o$.

The squared magnitude function (49) becomes

$$|H(e^{j\omega T})|^2 = \cfrac{1}{1 + \cfrac{\tan^{2n} \dfrac{\omega T}{2}}{\tan^{2n} \dfrac{\pi}{8}}} \tag{59}$$

The appropriate value of $n$ in (59) is $n = 4$, obtained by setting $\omega T = 72^o$ and $|H(e^{j\omega T})|^2$ to .01, thus satisfying the 20 db attenuation condition. The 8 poles in the $p$ plane are found from equation (57). Equation (58) can now be used to find the $z$ plane poles shown in Fig. 16, which also shows the $2n$ zeros located at $z = -1$, which are directly derivable from equation (50). The squared magnitude function is thus completely specified as pole-zero placements in the $z$ plane.

In the Appendix, an analysis is made of the necessary relations between an assumed squared magnitude function and the digital filter specified by that function. It is shown that, in order for a filter to be realizable, any pole inside the unit circle (for example $z_4$ in Fig. 16), must have a mate outside the unit circle of inverse magnitude and the same angle. Thus, if $z_4 = r\,e^{j\psi}$, there must be a pole (in this case $z_8$) given by $\dfrac{1}{r} e^{j\psi}$. In addition, all poles must occur in complex conjugate pairs. Therefore, the digital filter derived from Fig. 16 has the conjugate poles $z_4$, $z_5$ and $z_3$, $z_6$.

The above argument holds for the zeros as well including the special case of zeros on the real axis. In Fig. 16, all 8 zeros occur at $z = -1$. The derived filter has 4 zeros at $z = -1$.

If the squared magnitude function is given by

$$|H(e^{j\omega T})|^2 = \cfrac{1}{1 + \epsilon^2 V_n^2 \left[ \cfrac{\tan \dfrac{\omega T}{2}}{\tan \dfrac{\omega_c T}{2}} \right]} \tag{60}$$

then it can be shown that the poles of $p = \dfrac{z-1}{z+1}$ lie on an ellipse in the $p$ plane which has the same properties as the Chebyshev ellipse of Fig. 14. Using the notation of Section 2f and Fig. 14, the $p$ plane components can be written

$$x = a\,\tan\,\frac{\omega_c T}{2}\,\cos\theta$$

$$y = b\,\tan\,\frac{\omega_c T}{2}\,\sin\theta \tag{61a}$$

20

Substituting (61a) into (53) yields

$$
u = \frac{2\left(1 - a \tan \dfrac{\omega_c T}{2} \cos \theta\right)}{\left(1 - a \tan \dfrac{\omega_c T}{2} \cos \theta\right)^2 + b^2 \tan^2 \dfrac{\omega_c T}{2} \sin^2 \theta} - 1
$$

$$
v = \frac{2b \tan \dfrac{\omega_c T}{2} \sin \theta}{\left(1 - a \tan \dfrac{\omega_c T}{2} \cos \theta\right)^2 + b^2 \tan^2 \dfrac{\omega_c T}{2} \sin^2 \theta}
$$

(61b)

Figure 17 shows the z plane mapping for $a \tan \dfrac{\omega_c T}{2} = .5$ and $b \tan \dfrac{\omega_c T}{2} = 1$. The ellipse of Fig. 14 maps into the cardioid-like curve of Fig. 17 and the inner circle of Fig. 14 maps into the right-hand circle of Fig. 17. The outer circle of Fig. 14 maps into a circle of infinite radius, shown by the straight line of Fig. 17. The points shown on the mapped ellipse of Fig. 17 are the actual computed points from equation (61b).

h.    Technique 3 - Design of Digital Filters Using Bilinear Transformation of Continuous Filter Function

Another approach, using design directly in the s plane will now be considered. Suppose we have a stable analog filter described by H(s). Its frequency response is found by evaluating H(s) at points on the imaginary axis of the s plane. If in the function H(s), s is replaced by a rational function of z which maps the imaginary axis of the s plane onto the unit circle of the z plane, then the resulting H'(z), evaluated along the unit circle, will take on the same set of values as H(s) evaluated along the imaginary axis.

Of course, this does not mean the functions are the same, for the frequency scales are distorted relative to one another. This is illustrated by the simplest rational function which maps the $j\omega$ axis onto the unit circle,

$$
s \rightarrow \frac{z - 1}{z + 1} .
$$

(62)

Let the analog frequency variable be $\omega_A$, and let the digital frequency variable be $\omega_D T$. Then the functions $H(\omega_A)$, $H'(\omega_D T)$ take on the same values for

21

$$\omega_A = \tan \frac{\omega_D T}{2} \qquad (63)$$

Note that the transformation (62) leads to a ratio of polynomials in z. Since it maps the left half of the s plane onto the inside of the unit circle we can be sure that it will always yield for H'(z) a realizable, stable digital filter.

Equations (62) and (63) yield a technique for designing a digital filter by analog techniques. The procedure is as follows:

(1) Note the critical frequencies and ranges (pass or stop band, maximum attenuation point, etc.) of the desired digital filter, and call them $\omega_{D_i} T$. Compute a new set of frequencies, $\omega_{A_i}$, by

$$\omega_{A_i} = \tan \frac{\omega_{D_i} T}{2} \qquad . \qquad (64)$$

(2) Design a transfer function H(s) with the properties of the digital filter at the new frequencies and ranges. There is, of course, no need to synthesize H(s).

(3) Replace s by $\frac{z-1}{z+1}$ in H(s), and perform the algebra necessary to express the resulting H'(z) as a ratio of polynomials - this yields the desired digital filter.

This technique is illustrated by the following example, in which we design a digital filter for a 10 kc sampling rate, which is flat to 3 db in the pass band of 0 to 1000 cps, and which is more than 10 db down at frequencies beyond 2000 cps. The filter must be monotonic in pass and stop bands.

From Fig. 12 we see that a Butterworth filter meets the above requirement in the analog domain. The critical frequencies are $\omega_{D_1} T = 2\pi \times .1$ and $\omega_{D_2} T = 2\pi \times .2$.

(1) Compute $\omega_{A_1}$, $\omega_{A_2}$

$$\omega_{A_1} = \tan \frac{2\pi \times .1}{2} = 0.3249$$

$$\omega_{A_2} = \tan \frac{2\pi \times .2}{2} = 0.7265$$

22

(2)    We design a Butterworth filter with 3 db point at $\omega_c = \omega_{A_1} = .3249$. $\omega_{A_2}/\omega_c = 2.235$. To find the order $n$ we solve $1 + (2.235)^{2n} = 10$ and obtain $n = 2$. A second order Butterworth filter with $\omega_c = .3249$ has poles at $s = .3249 \times (-.707 \pm j\,.707) = -.23 \pm j\,.23$, and no zeros.

$$H(s) = \frac{s_1 s_2}{(s + s_1)(s + s_2)} = \frac{2 \times .23^2}{(2 + .23)^2 + (.23)^2} = \frac{.1058}{s^2 + .46\,s + .1058}$$

(3)    We replace $s$ by $\frac{z-1}{z+1}$, yielding $H'(z)$.

$$H'(z) = \frac{.1058}{\left(\frac{z-1}{z+1}\right)^2 + .46\left(\frac{z-1}{z+1}\right) + .1058}$$

$$H'(z) = \frac{.1058(z^2 + 2z + 1)}{1.5658z^2 - 1.7884z + .6458}$$

This is the required digital filter. It requires 3 multiplications per output point, or if DC gain can be tolerated, only two multiplications.

Problem:    Design a digital filter passing from 0 to 100 cps with 1/2 db ripple, which falls off monotonically to at least $-19$ db at 183 cps. Use 1000 cps sampling rate.

(1)    The critical frequencies 100 and 183 cps are transformed to analog frequencies.

$$\omega_c = \tan\frac{2\pi \times 100}{2 \times 1000} = \tan 18^o = .32492$$

$$\omega_s = \tan\frac{2\pi \times 183}{2 \times 1000} = .6498 \approx 2\omega_c$$

(2)    We now design an analog filter of the Chebyshev variety. One-half db ripple corresponds to $\epsilon^2 = .1220184$. To find the required order we solve $1 + \epsilon^2 V_n^2(\omega_s/\omega_c) = 10^{1.9}$. The lowest order $n$ satisfying this relationship is $n = 3$.

A unity bandwidth, 1/2 db ripple Chebyshev filter is

23

$$H_1(s) = \frac{\text{constant}}{s^3 + 1.252913s^2 + 1.5348954s + .7156938}$$

Replacing $s$ by $s/\omega_c$ yields

$$H(s) = \frac{.0255842155}{s^3 + .4127346s^2 + .16656307s + .0255842155}$$

where the constant has been adjusted for unity gain at $s = 0$.

(3)     We replace $s$ by $\frac{z-1}{z+1}$, giving for the digital filter desired, after multiplying numerator and denominator by $(z+1)^3$:

$$H'(z) = \frac{.0255842155\,(z^3 + 3z^2 + 3z + 1)}{1.60488218z^3 - 3.169418z^2 + 2.44628634z - .728243953}$$

which is the required digital filter design.

It is worth noting a useful geometric interpretation of Step 3. Replacing $s$ by $\frac{z-1}{z+1}$ is a mapping of points in the $s$ plane onto points in the $z$ plane. The following short table gives the correspondence of some critical points in the $s$ and $z$ planes

| s plane | z plane |
|---|---|
| $0 + j\,0$ | $1 + j\,0$ |
| $\infty$ | $-1 + j\,0$ |
| $0 + j\,1$ | $0 + j\,1$ |
| $0 - j\,1$ | $0 - j\,1$ |
| $-1 + j\,0$ | $0 + j\,0$ |
| point on real axis | point on real axis |
| point on imaginary axis | point on unit circle |
| point on any line | point on circle passing through $-1 + j\,0$ |

A very similar mapping has been found useful in some applications, and graph paper which performs the transformation can be purchased under the name "Smith Chart". To perform the mapping of our application we take a conventional Smith Chart and rotate it $180^o$, giving a chart like Fig. 18.

The location of any point $-a + j\,b$ in the $s$ plane (left half) is used to find the corresponding location in the $z$ plane as follows:

24

(1)    Locate  a,  a point along the centerline.  All points along the circle passing through this point correspond to points in the  s  plane with real part = −a.

(2)    Locate  b,  a point along the perimeter of the outer circle.  For b > 0 use the top semicircle; for b < 0  use the lower semicircle.  The circular arcs passing through this point correspond to points in the  s  plane with imaginary part b.

(3)    The intersection of the circle with the circular arc is the point in the z  plane corresponding to  −a + j b  in the  s  plane.

The Smith Chart is useful when the function in the  s  plane is known in terms of poles and zeros or poles and residues, especially when the  z  plane representation is desired in that form.

Example:  Design of a digital high-pass filter with stop band  (0 - 500 cps) attenuation greater than  36 db  and pass band (above  660 cps) ripple of  1.25 db. Sampling rate is  2.5 kc.

(1)    The critical frequencies are transformed to analog,  giving as the stop band limit,  .72654 rad/sec, and as the pass-band limit,  1.09 rad/sec.

(2)    The specifications are met with a fourth order elliptic filter.  The design of elliptic filters is covered in the literature[17] and only the result is given here.  The poles are at  s  =  −1.1915812 ± j1.5528835, and −.11078815 ± j1.09445605,  and the zeros are at  s  =  0 (double), and ± j0.69117051.

These are located on a Smith Chart in Fig.  18.  Using a ruler and protractor the zeros in the  z  plane are found to be at  z  =  1 (double), and $e^{\pm j69.3^o}$ and the poles are found to be at  z  =  .586 $e^{\pm j131.6^o}$  and  .895 $e^{\pm j90.6^o}$.  The function of z  defining the filter is thus

$$H(z) = \frac{(z - 1)^2 (z^2 - .707z + 1)}{(z^2 + .777z + .3434)(z^2 + .01877z + .801)}$$

A prime difficulty with the Smith Chart method, illustrated by this example, is that the poles cannot be located with great accuracy.  In compensation, a good deal of insight into the operation of the digital filter is gained in the course of the design.  Where greater accuracy is needed, the  z  plane poles can be computed from the  s  plane poles using

$$z = \frac{1 + s}{1 - s}$$

which is the inverse of equation (62).

The transformation $s \rightarrow \dfrac{z-1}{z+1}$ is not the only rational function of $z$ which maps the imaginary axis of the $s$ plane onto the unit circle. For example, another such transformation is

$$s \rightarrow \frac{z^2 - 2z \cos \psi_o T + 1}{z^2 - 1} \tag{65}$$

For this transformation the imaginary axis of the $s$ plane maps onto the top arc of the unit circle, and also onto the bottom arc. The origin of the $s$ plane maps onto the two points $e^{\pm j \psi_o T}$.

Thus, equation (65) maps a frequency function $H(\omega_A)$ into $H'(\omega_D T)$ with

$$\omega_A = \frac{\cos \psi_o T - \cos \omega_D T}{\sin \omega_D T} \tag{66}$$

This means that equation (65) transforms a low-pass $H(\omega_A)$ into a band pass $H'(\omega_D T)$. Equation (65) can thus be used to design band-pass digital filters as follows:

(1)    Decide on a center frequency $\psi_o T^*$ for the digital filter. This may be forced by the specifications or it may be available to simplify the choice of other parameters. Compute the critical frequencies of the desired analog filter from the critical frequencies in the specification of the digital filter using Eq. (66). Equation (66) will often yield negative frequencies, which is alright since $H(\omega_A)$ will be an even function of $\omega_A$.

(2)    Design an analog filter $H(s)$ with the translated specifications. It is likely that one or more of the specifications will be superfluous.

(3)    Replace $s$ by

$$s = \frac{z^2 - 2z \cos \psi_o T + 1}{z^2 - 1}$$

---

*All that is ever really needed is $\cos \psi_o T$.

26

in $H(s)$, and perform the required algebra to manipulate the resulting $H'(z)$ into a ratio of polynomials; this is the required filter.

One example will probably suffice to illustrate the method.

Problem: Design a digital band-pass filter for a 1000 cps sampling rate, to pass 100 to 400 cps with ripple free attenuation between 0 and 3 db. At 45 and 450 cps the filter must be at least 20 db down, and must fall off monotonically beyond both frequencies.

(1)     $\psi_o T$ can be chosen so the two analog 3 db points are negatives of each other. If the digital 3 db points are $L_1$ and $L_2$, we can see from (66) that $\psi_o T$ should be chosen so that

$$\cos \psi_o T = \frac{\cos \frac{1}{2}(L_1 + L_2)}{\cos \frac{1}{2}(L_1 - L_2)} \tag{67}$$

Using (67) yields $\cos \psi_o T = 0$ for this case. This means that the transformation from digital to analog critical frequencies becomes

$$\omega_A = -\cot \omega_D T$$

The 3 db points now translate to

$$\omega_{3db} = \pm 1.3764$$

The 20 db points are not equal in magnitude. They are

$$\omega_{s_1} = -3.442$$

$$\omega_{s_2} = 3.078$$

(2)     The problem is now to design a monotonic filter with 0-3 db in the region $0 < \omega < 1.3764$. The filter must be 20 db down by $\omega = 3.078$, which will automatically satisfy the requirement at $\omega = 3.442$. A Butterworth design seems to be called for, with $\omega_c = 1.3764$.

For $\frac{\omega}{\omega_c} = 2.23$ we demand 20 db attenuation. We calculate the order n:

$$1 + (2.23)^{2n} = 100$$

It is clear that $n = 3$ will suffice. A unity bandwidth Butterworth filter of order 3 is

$$H_1(s) = \frac{K}{s^3 + 2s^2 + 2s + 1}$$

$H(s)$ is found by replacing $s$ by $\frac{s}{1.3764}$:

$$H(s) = \frac{2.6075581}{s^3 + 2.7528s^2 + 3.788954s + 2.6075581}$$

(3)     To find the required digital filter we let $s = \frac{z^2 + 1}{z^2 - 1}$ in $H(s)$. Note that since this is going to yield a function of $z^2$, the resulting digital filter will be quite simple.

$$H'(z) = \frac{2.6075581z^6 - 7.8226743z^4 + 7.8226743z^2 - 2.6075581}{10.1493121z^6 - 5.8588283z^4 + 4.2809203z^2 - 0.5714041}$$

If the gain of the filter is not important, this can be programmed with 3 multiplications per output point, plus a moderate number of additions.

It should be obvious how the techniques of this section can also be used to design high-pass and band-elimination filters.

i.     Technique 4 - Frequency Sampling Technique

The difference equation

$$y(nT) = x(nT) - x(nT - mT) \tag{68}$$

has the $z$ transfer function $1 - z^{-m}$, which has $m$ zeros equally spaced around the unit circle, at points

$$z_k = e^{j2\pi \frac{k}{m}} \quad ; \quad k = 0, 1, \ldots, m - 1 \quad . \tag{69}$$

If, in equation (68), the subtraction is replaced by an addition, the transfer function becomes $1 + z^{-m}$, for which the zeros are also equally spaced around the unit circle, at

$$z_k = e^{j2\pi(\frac{k + 1/2}{m})} \quad ; \quad k = 0, 1, \ldots, m - 1 \quad . \tag{70}$$

The magnitude versus frequency curves of these filters repeat with period $\frac{2\pi}{m}$ radians, and the filters are often referred to as comb filters. These filters can be incorporated into an especially appealing type of design. Before presenting this design, let us examine the practical significance of (68). If successive values of $x(nT)$ are thought of as contents of registers in computer memory, it is clear that $m$ registers must be set aside for buffer storage in order to execute (68). This is usually a substantial amount of memory compared to that needed for execution of second order difference equations. Thus possible practical use of the filters we are about to describe is limited to systems where the necessary memory is available, or to systems where many filters share a common input. It is important to note that the delays implied by (68) can be effected by digital delay lines, which are presently relatively cheap forms of memory.

A simple resonator can be placed in cascade with the comb filter. Let the resonator be of the type considered in Section 2d, case 4, except that the poles lie directly on the unit circle. Further let the angle, $\omega_r$, of a resonator pole be such that the pole is coincident with a zero of the comb filter.

$$\omega_r = \begin{Bmatrix} \dfrac{2\pi k}{m} \\ \dfrac{2\pi(k + 1/2)}{m} \end{Bmatrix} \text{ for a comb filter of the } \begin{Bmatrix} \text{first} \\ \text{second} \end{Bmatrix} \text{ type} \tag{71}$$

The poles of the resonator cancel the $k^{th}$ zero of the comb filter, and its conjugate. In what follows, we shall refer to the resonator which is used to cancel the $k^{th}$ zero as the $k^{th}$ elemental filter.

The cascade of an elemental filter with a comb filter is a composite filter with the following properties:

(1) The impulse response is of finite duration, $mT$.

(2) The magnitude versus frequency response is

$$|H(e^{j\omega T})| = \left| \frac{\sin m\omega T/2}{\cos \omega T - \cos \omega_r T} \right| \tag{72}$$

which is zero at all the radian frequencies for which the comb filter is zero, except at $\omega_r$. The magnitude at $\omega_r$ is $\frac{m}{2} \csc \omega_r T$.

(3) The phase versus frequency is exactly linear except for discontinuities of $\pi$ radians. These discontinuities occur where the magnitude response is zero.

(4) The phase difference between two composite filters with resonant frequencies $\omega_r$ and $\omega_{r+1}$ is $\pi$ for $\omega_r < \omega < \omega_{r+1}$ and is zero outside these bounds.

(5) The amplitude of any composite filter is zero at the resonant frequencies of all the other composite filters.

As $m$ is made large, the magnitude response of a cascaded filter becomes like

$$\left[ \frac{\sin(\omega - \omega_r)T}{(\omega - \omega_r)T} + \frac{\sin(\omega + \omega_r)T}{(\omega + \omega_r)T} \right]$$

in shape. These properties suggests that any desired magnitude response could be obtained by adding together the weighted outputs of cascaded comb and elemental filters, just as any "band-limited" time function can be formed from a weighted sum of delayed $\frac{\sin t}{t}$ functions. Let us examine this idea, which we call frequency sampling, in some detail.

A sufficiently "narrow band" frequency response function (one for which the frequency response is a sufficiently smooth function of frequency) is sampled at equally spaced points, with radian frequencies:

$$\omega_k = \frac{2\pi k}{m} \text{ or } \frac{2\pi(k + 1/2)}{m} \quad ; \quad k = 0, 1, \ldots, m - 1$$

depending on which kind of comb filter will be used. Let the sample value of the amplitude at frequency $\omega_k T$ be $W_k$. An elemental filter of resonant frequency $\omega_k$, cascaded with a comb filter of delay $mT$ and a gain of $W_k \sin \omega_k T$ are used to provide an "elemental frequency response" of $W_k$ at radian frequency $\omega_k T$ and zero at the other sampling frequencies.

Since the phases at resonance of the consecutive elemental filters differ by $\pi$, the gains of the odd numbered elemental filters are to be multiplied by $-1$. The desired input to the filter is applied to the comb filter, which is shared among all

the elemental filters, followed by the gains (and sign changers for odd numbered elemental filters). The outputs of all the elemental filters, with proper gains, are added together to give the desired filter output. The resulting filter has an impulse response of duration $mT$, a frequency response with linear phase, and an amplitude response which agrees with specifications at the sampling frequencies and connects the sampling points smoothly. The variety of filters which can be programmed with this technique is quite large.

There are some practical problems to be considered before the frequency sampling method is applied. For one thing, the resonant poles of an elemental filter cannot exactly cancel the zeros of a comb filter because of quantization. Thus it is wise to move both the zeros of the comb filter and the poles of the elemental filters slightly inside the unit circle, with a radius of something like $e^{-aT} = 1 - 2^{-26}$.

We have successfully programmed filters with the poles and zeros at radii ranging from $1 - 2^{-12}$ to $1 - 2^{-27}$, with little change in the behavior of the filter.

Another change, while not necessary, is useful to keep in mind for band-pass filters. In the pass band it is common for the samples $W_k$ to be equal. Thus it would be desirable if all the elemental filters had the same gains at resonance. If a zero is put at $(\cos \omega_k T)\, e^{-aT}$, the gain of each elemental in cascade with the comb filter becomes $m/2$. This has a slight effect on the magnitude and phase response, negligible for large $m$. The modified comb filter $z$ transform thus becomes

$$H(z) = 1 - e^{-maT}\, z^{-m} \tag{73}$$

and the modified $k^{th}$ elemental filter becomes

$$H_k(z) = \frac{1 - e^{-aT} \cos \omega_k T\, z^{-1}}{1 - 2\, e^{-aT} \cos \omega_k T\, z^{-1} + e^{-2aT}\, z^{-2}} \tag{74}$$

It is worth noting that the introduction of the additional zero does not require another multiplication since twice the numerator coefficient is also present in the denominator. The response of a filter of the form of equations (73), (74) is shown in Fig. 19.

31

### Example: Bank of Band Pass Filters

It was desired to design a bank of band-pass filters (with a common input), each 400 cps wide, covering the band 300 cps to 3100 cps. The filters are to be as selective as possible but with minimum ringing time. A further requirement is that the contiguous filters cross at −3 db of the midband gain. None of the standard designs had satisfactory selectivity combined with short ringing.

The filters chosen were frequency sampling filters, each composed of seven elemental filters. The consecutive zeros were 100 cps apart. Since the sampling rate was 12.5 kc, m was 125. The general form of such a filter has z transform

$$H(z) = \left(1 - e^{-maT} z^{-m}\right) \sum_{k=r}^{r+6} (-1)^k \frac{1 - e^{-aT} \cos \frac{2\pi k}{m} z^{-1}}{1 - 2e^{-aT} \cos \frac{2\pi k}{m} z^{-1} + e^{-2aT} z^{-2}} W_k \quad . \quad (75)$$

The design of the filter is completely specified by choosing r and the set of $W_k$ in (75). Since 3 db crossovers 400 cps apart were required, $W_{r+1}$ and $W_{r+5}$ were chosen to be .707. The three center terms had $W_k = 1$. The end term gains, $W_r$ and $W_{r+6}$ were found empirically to be .221 for satisfactory out of band rejection.

The design of the 300-700 cps filter is illustrated in Fig. 20, and the experimental frequency response of it and the next higher filter (700-1100 cps) are shown in Fig. 21.

32

SECTION 3

Quantization Noise of Digital Filters

When a digital filter is realized with a digital arithmetic element, as is the case with a computer, additional considerations are necessary to describe the performance of the filter. There are three obvious degradations: 1) quantization of the coefficients of the difference equation, 2) quantization of the input, and 3) quantization of the results of computations. The first two effects, although important, are simple to understand. Quantization of the coefficients changes them to slightly different coefficients. This happens once and for all, resulting in a new, slightly different filter. For very high Q filters this may be important; even instability may result. Quantization of the input is equivalent to adding a noiselike term which has been well described in the literature. We rely heavily on the results of Bennett[18] in treating this and similar effects of quantization in a statistical manner.

Quantization of results of computation is more complicated because these results are used in later computations, and thus the effect of the error on future computations must be understood. Let us first note that quantization of the results cannot be avoided because after each iteration of the difference equation, the number of bits required for exact representation of the result increases by about as many bits as in the representation of the coefficients. Thus, without quantization, the number of bits required would grow without bound.

In the following, we define quantization as the replacement of the exact value of a quantity by the value of the nearest of a set of levels differing by steps of $E_o$. Thus, the maximum error introduced by a quantization is $E_o/2$, and, except for a few degenerate cases, the mean squared error is $E_o^2/12$.

Figure 22 shows a representation of a digital filter in which the output is quantized before being used in further iterations.

We can write a "linear" difference equation describing this device if we represent the quantization error by $v(nT)$.

$$r(nT) = v(nT) + \sum_{i=0}^{N} a_i \, x(nT - iT) + \sum_{i=1}^{M} b_i \, r(nT - iT) \tag{76}$$

This equation has a z transform form:

$$R(z) = V(z) + \sum_{i=0}^{N} a_i z^{-1} X(z) + \sum_{i=1}^{M} b_i z^{-i} R(z) \tag{77}$$

$$R(z) = \frac{V(z) + \sum_{i=1}^{N} a_i z^{-i} X(z)}{1 - \sum_{i=1}^{M} b_i z^{-i}} \tag{78}$$

We notice that the $z$ transform of the output consists of two terms, one of which is the desired output. The other term depends only on the poles of the filter and on the noise sequence $v(nT)$.

In what follows, assume that the input to the filter is of such level that the output with no quantization noise has a mean squared value of unity. Assume that this output is large compared to $E_0$, so that the samples $v(nT)$ are independent and uniformly distributed from $-E_0/2$ to $E_0/2$[18]. Let us call the denominator of the right side of (78) $Q(z)$. Our aim is to determine the mean squared value of the noise term of (78) in terms of $E_0$, the quantization step size.

For this determination, the two-sided $z$ transform[13] of the autocorrelation function of a sequence is needed. If a one-sided sequence has $z$ transform $A(z)$ then its autocorrelation function has a two-sided $z$ transform $A(z) A(\frac{1}{z})$. It follows that a sequence with $z$ transform $V(z)/Q(z)$ has an autocorrelation function whose $z$ transform is the ratio of the $z$ transforms of the autocorrelation functions of $v(nT)$ and $q(nT)$.

We are really interested in a normalized autocorrelation function,

$$\lim_{k \to \infty} \frac{1}{k} \sum_{i=0}^{k-1} g(iT) g(nT + i\,T)$$

which, for $v(nT)$ is the sequence

$$A_v(nT) = 0, \ldots, 0, E_0^2/12, 0, \ldots, 0, \ldots$$

with $z$ transform $A_v(z) = E_0^2/12$.

For the noise output, the normalized autocorrelation function has $z$ transform:

$$\frac{E_0^2/12}{Q(z) Q(\frac{1}{z})}$$

The mean squared output noise is, of course, given by the coefficient of $z^0$ in the $z$ transform of its autocorrelation function. For a two-sided $z$ transform this coefficient is given by

$$M.S.O.N. = \frac{E_o^2}{12}\left(\sum \text{ residues of } \frac{1}{zQ(z) \, Q(\frac{1}{z})}\right) \tag{79}$$

where only the residues at poles inside the unit circle are to be included in the sum.

Example:

Consider a one pole filter with $H(z) = \dfrac{1}{1 - az^{-1}}$. Then $\dfrac{1}{z \, Q(z) \, Q(1/z)}$ has a pole at $z = a$ and a residue of $\dfrac{1}{1 - a^2}$ at that pole. The mean squared output noise for a digital realization of this filter is proportional to this residue, which is plotted versus pole position in Fig. 23, with the constant of proportionality being $E_o^2/12$.

Two filters, one using 36 bit arithmetic and one using a variable number of bits fewer than 36, were simulated, with a common input to both filters, and with $H(z)$ as above. The 36 bit case was considered unquantized and the difference in the filter outputs was thus a good approximation to the quantization noise introduced by the less precise filter. The mean squared value of this noise was measured for a random noise input with 28 and 29 bit arithmetic, and for a sine wave input at about 0.1 of the sampling frequency, using 29 bit arithmetic. The measured results, normalized with respect to $E_o^2/12$, are shown along with the theoretical result in Fig. 23.

We have arrived at a very fortunate expression since we can quickly solve it for $(-\log_2 E_o)$ which is the number of bits of quantization needed below the output signal level, for a given amount of mean squared output noise. Say we require that the mean squared output noise be $F$ db below a unit output signal level. Then

$$F = 10 \log_{10}\left\{\frac{E_o^2}{12} \, (\Sigma \text{ residues})\right\} \tag{80}$$

$$b_{-1} = -\log_2 E_o = -.166 \, F - 1.79 + 1.66 \log_{10}\left(\Sigma \text{ residues of } \frac{1}{zQ(z) \, Q(\frac{1}{z})}\right) \tag{81}$$

$b_{-1}$ is the number of bits which must be retained below the unit signal level; an additional 3-5 bits ought to be retained above the unit signal level to protect against overflow.

35

The preceding description of quantization noise is valid for digital filters realized in the form of Fig. 1. If the realization is in the canonical form of Fig. 4 then quantization noise is added to $w(nT)$ rather than to $r(nT)$, since it is $w(nT)$ which is used in further computations. Figure 24 shows the digital arrangement of the canonical form. We write the two difference equations:

$$w(nT) = x(nT) + \sum_{i=1}^{M} b_i \, w(nT - iT) + v(nT) \tag{82}$$

$$r(nT) = \sum_{i=0}^{N} a_i \, w(nT - iT) \tag{83}$$

These may be $z$ transformed, giving

$$W(z) = (X(z) + V(z))/Q(z) \tag{84}$$

$$R(z) = P(z)\, W(z) \tag{85}$$

where

$$P(z) = \sum_{i=0}^{N} a_i \, z^{-i} \quad .$$

Combining these into a single equation

$$R(z) = X(z)\, \frac{P(z)}{Q(z)} + V(z)\, \frac{P(z)}{Q(z)} \tag{86}$$

we see that in the canonical representation the quantization noise is filtered by both the poles and the zeros of the filter. If desired, the procedures leading to equations (79), (80) and (81) could be repeated, giving as the mean squared output noise

$$M.S.O.N. = \frac{E_o^2}{12} \, \Sigma \text{ residues of } \left( \frac{P(z)\, P(\frac{1}{z})}{z Q(z)\, Q(\frac{1}{z})} \right) \tag{87}$$

and giving the number of bits required below a unit signal level as

$$b_{-1} = -.166F - 1.79 + 1.66 \log_{10}\left( \Sigma \text{ residues of } \frac{P(z)\, P(\frac{1}{z})}{z Q(z)\, Q(\frac{1}{z})} \right) \tag{88}$$

36

# APPENDIX
## REALIZABILITY OF DIGITAL FILTERS WITH CERTAIN SQUARED MAGNITUDE FUNCTIONS

In the following we shall find it useful to define polynomials of the form

$$a_0 z^k + a_1 z^{k-1} + \ldots + a_1 z + a_0 \quad ,$$

such that the coefficient of $z^r$ is equal to the coefficient of $z^{k-r}$, as mirror image polynomials of order $k$, and to summarize some of the properties of the polynomials.

(1)    A mirror image polynomial of order $k$ has roots which occur in reciprocal pairs for $k$ even.

Proof: Let $z$ be replaced by $1/z$ in the original M. I. P. and equate it to zero.

$$a_0 z^{-k} + a_1 z^{-k+1} + a_1 z^{-1} + a_0 = 0$$

If we multiply by $z^k$, which introduces no new roots to the equation, we see that the roots of the polynomial in $1/z$ are the same as the roots of the polynomial in z. Thus, the roots either occur in reciprocal pairs, or are self-reciprocals. For $k$ odd, one of the roots cannot be part of a reciprocal pair. This root is its own reciprocal, and since it must be real, it is either $+1$ or $-1$. We will generally not be interested in odd order M. I. P. 's.

(2)    The sum of mirror image polynomials of the same order is a M. I. P. of that order.

(3)    A mirror image polynomial of order $k$ plus $z^r$ times a mirror image polynomial of order $(k - 2r)$ is a mirror image polynomial of order $k$.

(4)    The product of mirror image polynomials is a mirror image polynomial.

(5)    A polynomial whose roots occur in reciprocal pairs is an M. I. P. (5) is proved by multiplying together the factors which are reciprocals, noting that each product is $=$ M. I. P. , and applying (4).

We shall use the above properties of mirror image polynomials to prove the existence of digital filters with certain squared magnitude functions. Suppose a

37

squared magnitude function, $F(\omega T)$, is given. We can always replace $\omega T$ by $-j \log z$, equivalent to $z = e^{j\omega T}$, to give a function $G(z)$ which is equal to $F(\omega T)$ when evaluated along the unit circle. For our purposes $G(z)$ must be a rational function of $z$ with real coefficients. We can guarantee this if, in the squared magnitude function, $\omega T$ only appears as part of the following expressions: $\sin^2 \frac{\omega T}{2}$, $\cos^2 \frac{\omega T}{2}$, $\tan^2 \frac{\omega T}{2}$, $\cot^2 \frac{\omega T}{2}$, $\sec^2 \frac{\omega T}{2}$, $\csc^2 \frac{\omega T}{2}$, and if these expressions are combined only by addition, subtraction, multiplication and division. This is because the squared triginometric functions of $\frac{\omega T}{2}$ yield rational functions of $z$, and rational functions form a field with multiplication and addition. The correspondence of squared trigonometric functions of $\frac{\omega T}{2}$ with rational functions of $z$ is given below:

<div align="center">

TABLE 1

$$\sin^2 \frac{\omega T}{2} \;\to\; \frac{(z-1)^2}{-4z}$$

$$\cos^2 \frac{\omega T}{2} \;\to\; \frac{(z+1)^2}{4z}$$

$$\tan^2 \frac{\omega T}{2} \;\to\; \frac{-(z-1)^2}{(z+1)^2}$$

$$\cot^2 \frac{\omega T}{2} \;\to\; \frac{-(z+1)^2}{(z-1)^2}$$

$$\sec^2 \frac{\omega T}{2} \;\to\; \frac{4z}{(z+1)^2}$$

$$\csc^2 \frac{\omega T}{2} \;\to\; \frac{-4z}{(z-1)^2}$$

</div>

Now let us assume that we have been given an $F(\omega T)$ with the preceding restrictions, found $G(z)$, and found all the poles and zeros of $G(z)$. To find a transfer function, $H(z)$, with squared magnitude function $F(\omega T)$, we should like to use the following procedure:

(1)    Discard any poles or zeros at the origin.

(2)     Put the remaining poles in one to one correspondence with each other in such a way that for each pair of poles the distance from one pole to any point on the unit circle is in constant ratio to the distance from that point on the unit circle to the other pole of the pair.

(3)     Repeat step 2 for the zeros.

(4)     Discard one of each corresponding pair of poles and zeros, making sure that the retained poles are all within the unit circle.

(5)     Form $H(z)$ from the retained poles and zeros only.

This procedure works only if steps 2 and 3 are possible. The magnitude of $H(z)$ is proportional to the product of the distances from the unit circle to retained zeros divided by the product of distances to the retained poles, and thus is proportional to the square root of $F(\omega T)$. Note that the singularities of $G(z)$ at the origin contribute nothing to a magnitude function since the distance from the origin to the unit circle in always one.

Steps 2 and 3 are possible if the poles (and zeros) occur in pairs whose locations are equal or, more commonly, conjugate reciprocals of each other, $re^{j\theta}$ and $\frac{1}{r}e^{j\theta}$. Since the singularities of $G(z)$ occur in conjugate pairs it is enough to require the roots to occur in equal or reciprocal pairs. By the following proof we show that the ratio of distances from any point on the unit circle to two singularities which are conjugate reciprocals is constant. Proof: Let the two fixed singularities be $re^{j\theta}$ and $\frac{1}{r}e^{j\theta}$. By the theorem of Appollonius the locus of points, the ratio of whose distance to two fixed points is constant, is a circle whose center is colinear with the two fixed points. Consider the ratios at the two points $e^{j\theta}$ and $e^{j(\theta+\pi)}$. The ratios are equal to $r$ at both points, and the only circle passing through both points whose center is colinear with the two fixed points is the unit circle. Thus, the unit circle is the circle of Apollonius, and the ratio of the distance to the singularities is constant.

The corresponding proof for equal singularities is trivial.

If after discarding poles or zeros at the origin the numerator and denominator of $G(z)$ become mirror image polynomials, it is possible by following the five step procedure given above to find $H(z)$ with squared magnitude function $F(\omega T)$*. We

---

*This is not strictly correct if the mirror image polynomials have simple roots on the unit circle, which are then their own conjugate reciprocals. Subsequent statements should be qualified by taking this possibility into account. However, this is a limiting case, unlikely to occur.

shall now enumerate a few types of $F(\omega T)$ which yield mirror image polynomials for numerator and denominator of $G(z)$.

Consider $F(\omega T)$ a rational function of $\sin^2 \frac{\omega T}{2}$. Then $G(z)$, by substitution from Table 1, is of the form:

$$G(z) \; = \; \frac{a_o\left[\dfrac{(z-1)^2}{-4z}\right]^n \; + \; a_1\left[\dfrac{(z-1)^2}{-4z}\right]^{n-1} \; + \; \cdots}{b_o\left[\dfrac{(z-1)^2}{-4z}\right]^m \; + \; b_1\left[\dfrac{(z-1)^2}{-4z}\right]^{m-1} \; + \; \cdots}$$

which can be put in the form

$$G(z) \; = \; \frac{(a_o(z-1)^2)^n + a_1((z-1)^2)^{n-1}(-4z) + a_2((z-1)^2)^{n-2}(-4z)^2 + \ldots)(-4z)^{m-n}}{b_o((z-1)^2)^m + b_1((z-1)^2)^{m-1}(-4z) + b_2((z-1)^2)^{m-2}(-4z)^2 + \ldots}$$

The $(-4z)^{m-n}$ contributes only poles or zeros at the origin and is discarded. Note that powers of $(z-1)^2$ are mirror image polynomials by property (5), and thus the entire numerator of $G(z)$ is a mirror image polynomial by property (3). The same reasoning holds for the denominator.

Exactly similar reasoning shows that rational functions of $\cos^2 \frac{\omega T}{2}$ also yield realizeable digital filters. Rational functions of $\tan^2 \frac{\omega T}{2}$ yield $G(z)$ of the form

$$G(z) \; = \; \frac{a_o(z-1)^{2n} + a_1(z-1)^{2(n-1)}(z+1)^2 + \ldots + a_n(z+1)^{2n}}{b_o(z-1)^{2m} + b_1(z-1)^{2(m-1)}(z+1)^2 + \ldots + b_m(z+1)^{2m}} \; (z+1)^{2(m-n)}$$

Here we note by repeated application of property (4) that again both numerator and denominator are mirror image polynomials and therefore a digital filter exists with the desired squared magnitude function. Again exactly similar reasoning suffices to extend the proof to rational functions of $\cot^2 \frac{\omega T}{2}$, $\sec^2 \frac{\omega T}{2}$ and $\csc^2 \frac{\omega T}{2}$.

Similar discussions show that rational functions of sums of products or ratios of the squares of the trig functions of Table 1, i.e., $(\sin^2 \frac{\omega T}{2} + \tan^4 \frac{\omega T}{2})$ also yield $G(z)$ which is a ratio of mirror image polynomials. Further extensions can be made, but we shall be content here with these few examples and techniques.

40

## ACKNOWLEDGEMENT

# REFERENCES

1. C. M. Rader, "Study of Vocoder Filters by Computer Simulation," J. Acoust. Soc. 36 1023(A), (1964).

2. R. M. Golden, "Digital Computer Simulation of a Sampled-Data Voice Excited Vocoder," J. Acoust. Soc. Am. 35 1358-1366, (1963).

3. B. Gold and C. M. Rader, "Bandpass Compressor: A New Type of Speech Compression Device," J. Acoust. Soc. Am. 36 1215, (1964).

4. C. M. Rader, "Vector Pitch Detection," J. Acoust. Soc. Am. 36 1963(L) (1964).

5. C. M. Rader, "Speech Compression Simulation Compiler," J. Acoust. Soc. Am. (A), (June 1965).

6. B. Gold, "Experiment With Speechlike Phase in a Spectrally Flattened Pitch-Excited Channel Vocoder," J. Acoust. Soc. Am. 36 1892-1894 (1964).

7. E. J. Kelly and M. J. Levin, "Signal Parameter Estimation for Seismometer Arrays," Tech. Report No. 339, Lincoln Laboratory, M. I. T., (8 Jan. 1964).

8. H. M. James, N. B. Nichols and R. S. Phillips, "Theory of Servo-Mechanisms," Rad. Lab. Ser. 25 Chap. 5 pp 231-261, (1947).

9. W. D. White and A. E. Ruvin, "Recent Advances in the Synthesis of Comb Filters," IRE Nat. Conv. Rec. 5, 186-199, (1957).

10. M. Lewis, "Synthesis of Sampled-Signal Networks," IRE Trans. on Circuit Theory, (March 1950).

11. R. M. Golden and J. F. Kaiser, "Design of Wideband Sampled-Data Filters," B. S. T. J. XLIII, No. 4, (July 1964).

12. J. Craig, unpublished notes, (1963).

13. J. R. Ragazzini and G. F. Franklin, "Sampled-Data Control Systems, (McGraw Hill, 1958).

14. R. M. Lerner, "Band-Pass Filters with Linear Phase," Proc. IEEE 52, 249-268, (1964).

15. E. A. Guilleman, "Synthesis of Passive Networks," (Wiley 1957).

16. L. Weinberg, "Network Analysis and Synthesis," (McGraw Hill 1962).

17. J. E. Storer, "Passive Network Synthesis,"(McGraw Hill 1957).

18. W. R. Bennett, "Spectra of Quantized Signals, "Bell System Technical Journal, New York, N. Y., 27, (July 1948), pp 446-472.
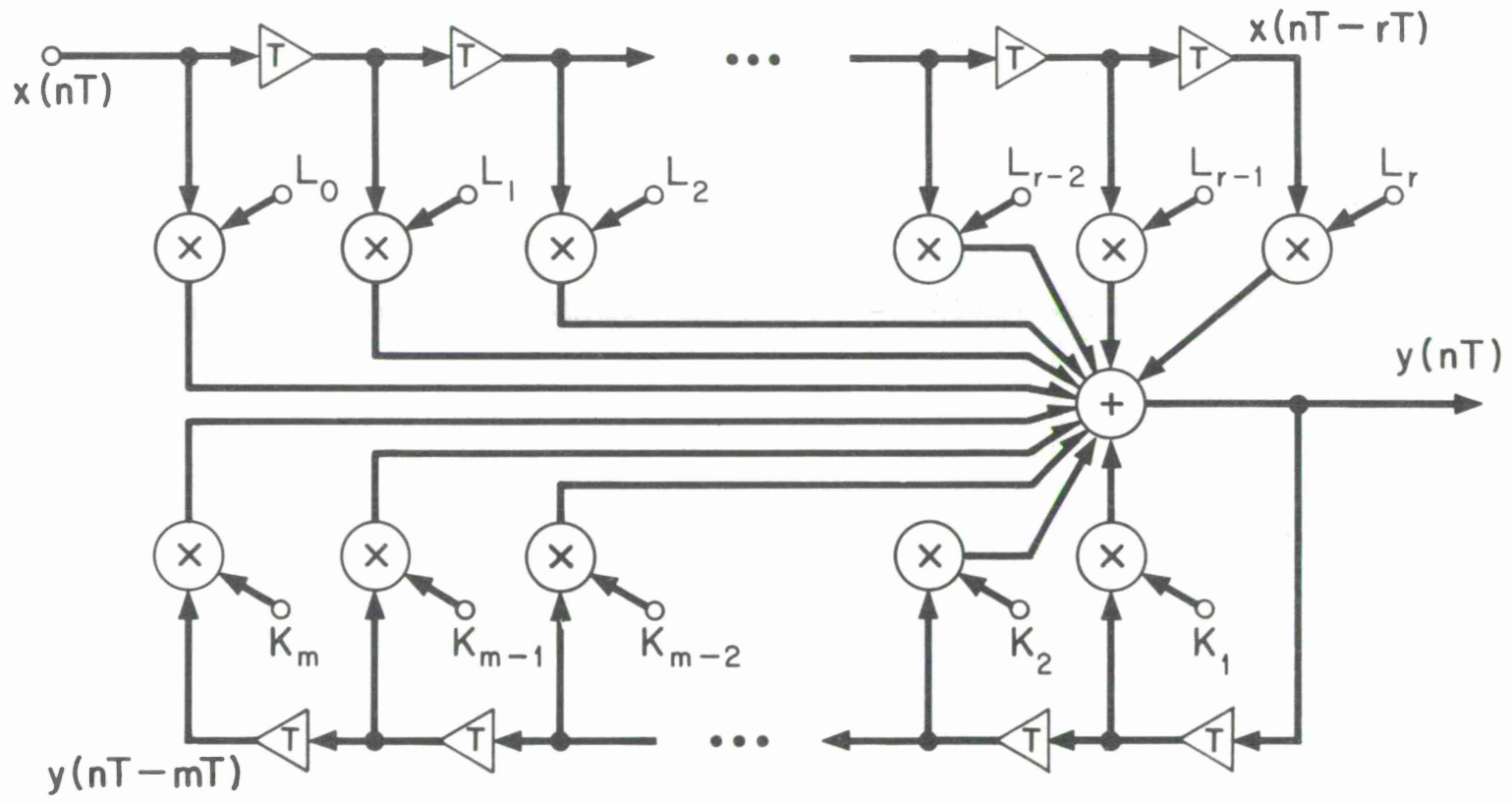
Fig. 1.    Pictorial representation of $m^{th}$ order linear difference equation.
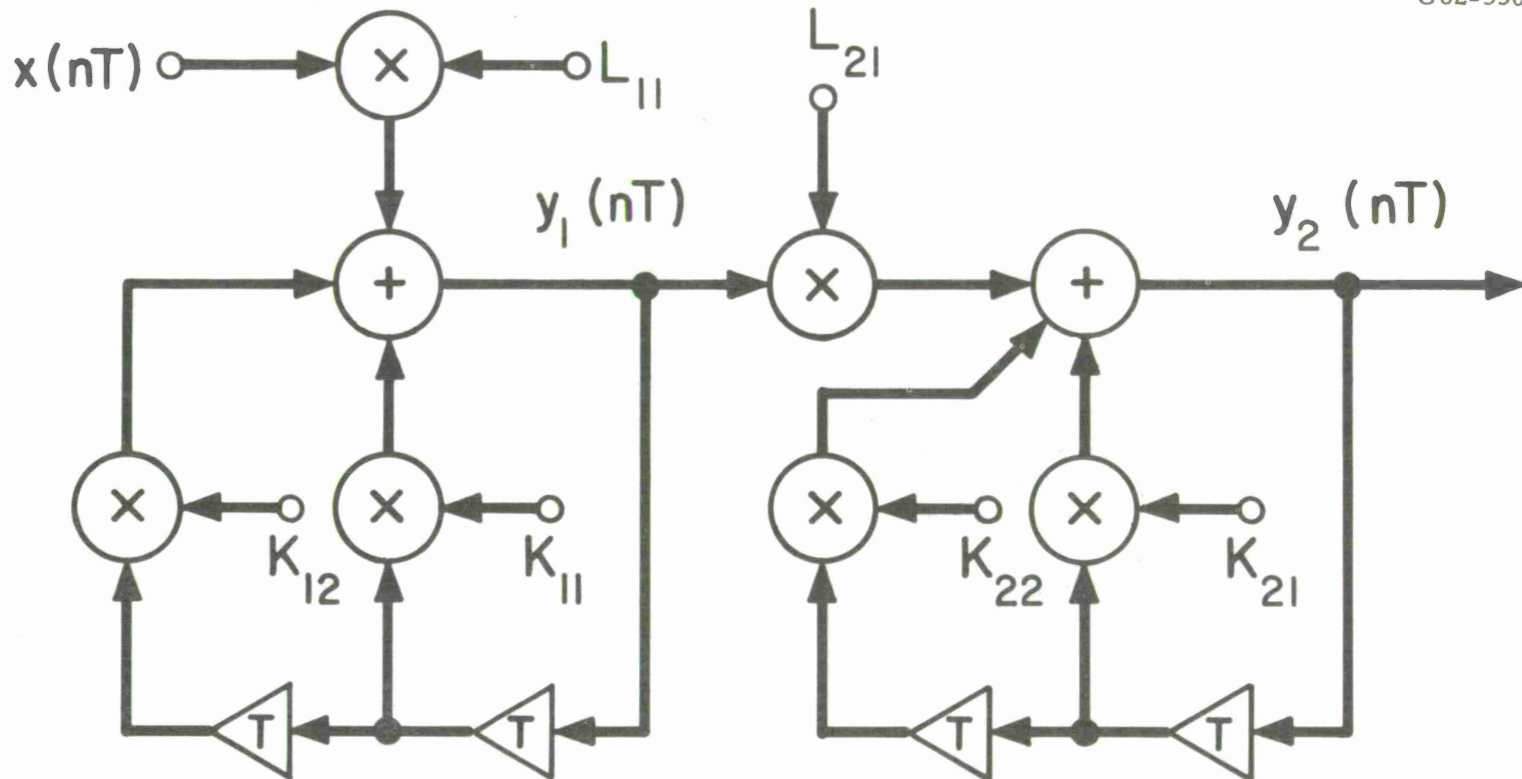
Fig. 2.    Serial arrangement of difference equations.
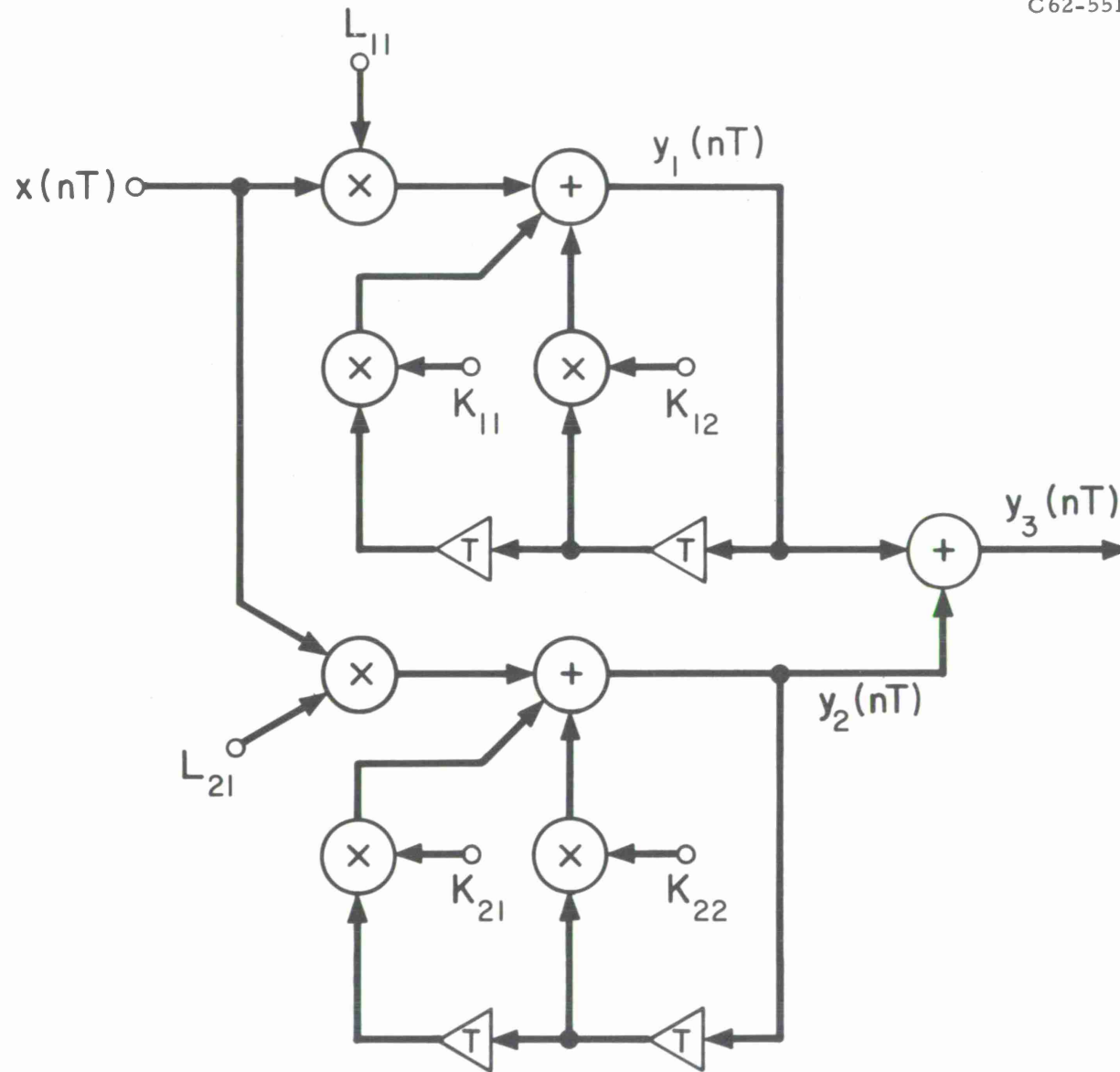
Fig. 3.    Parallel arrangement of difference equations.
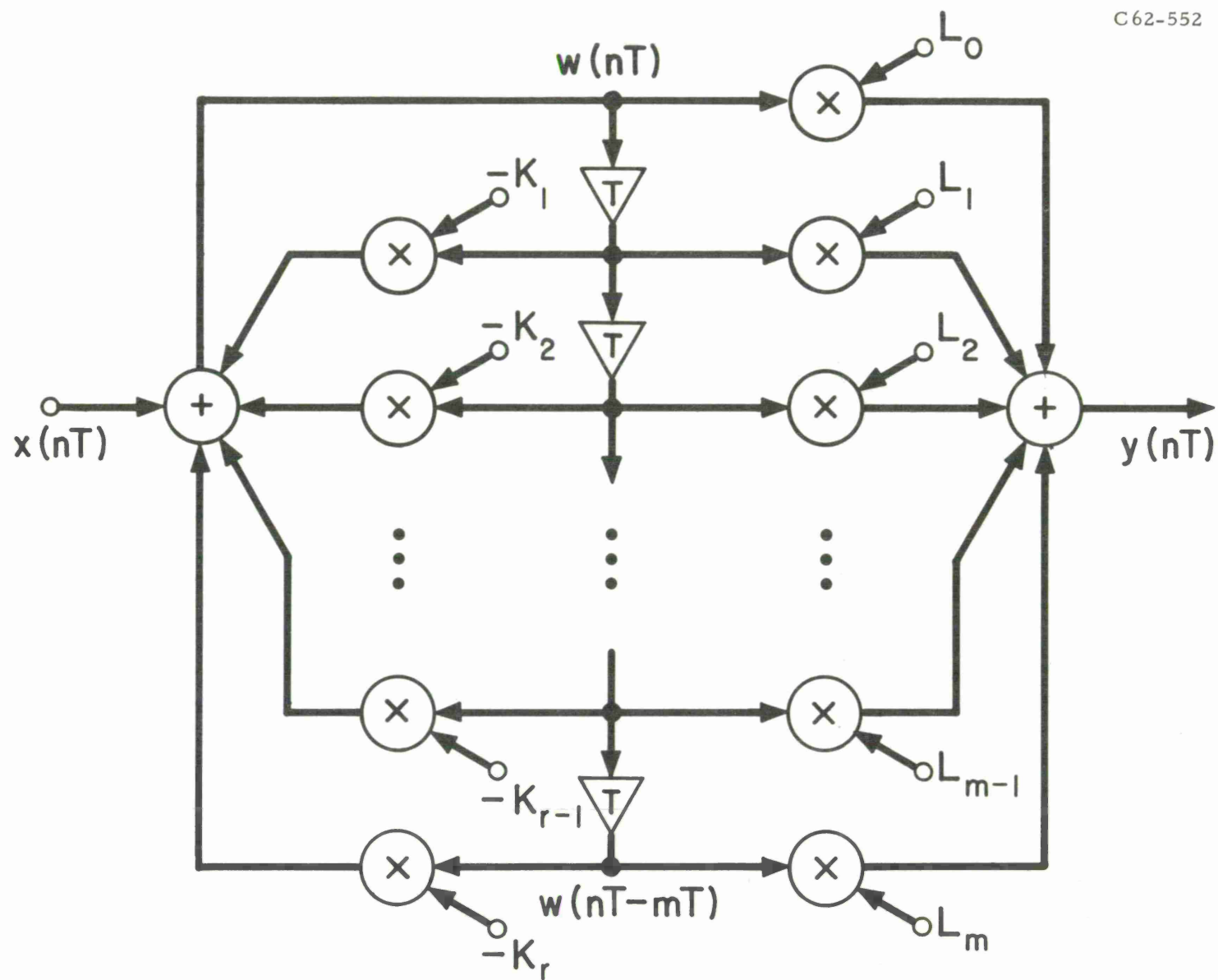
Fig. 4.    Alternate representation of digital filter (drawn for m = r).

$$\left|H(e^{j\omega T})\right| = \frac{R_1 R_2}{P_1 P_2 P_3}$$
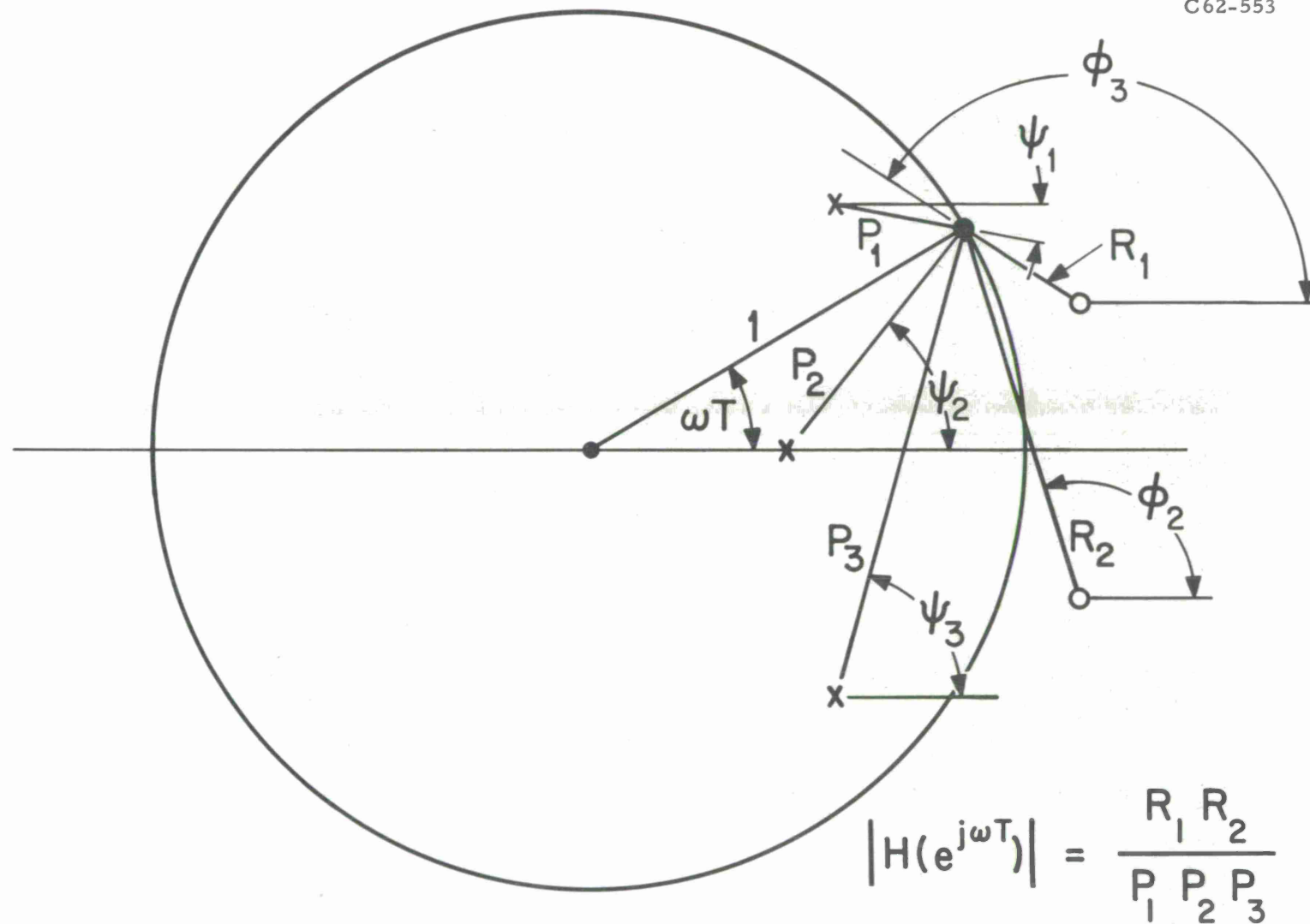
Fig. 5.    Geometric interpretation of digital filter frequency response function.
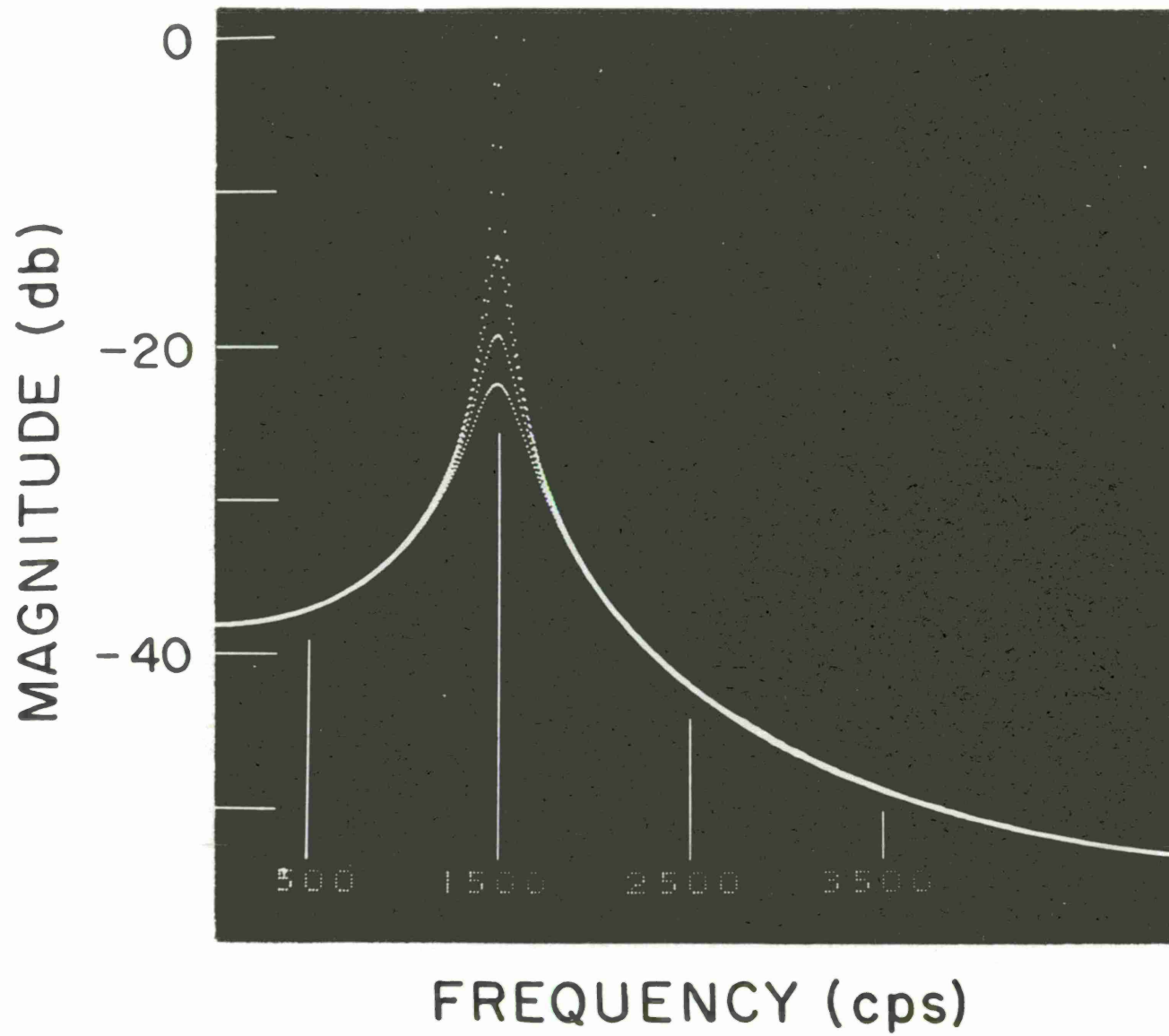
Fig. 6.    Response of digital resonator for several values of damping.
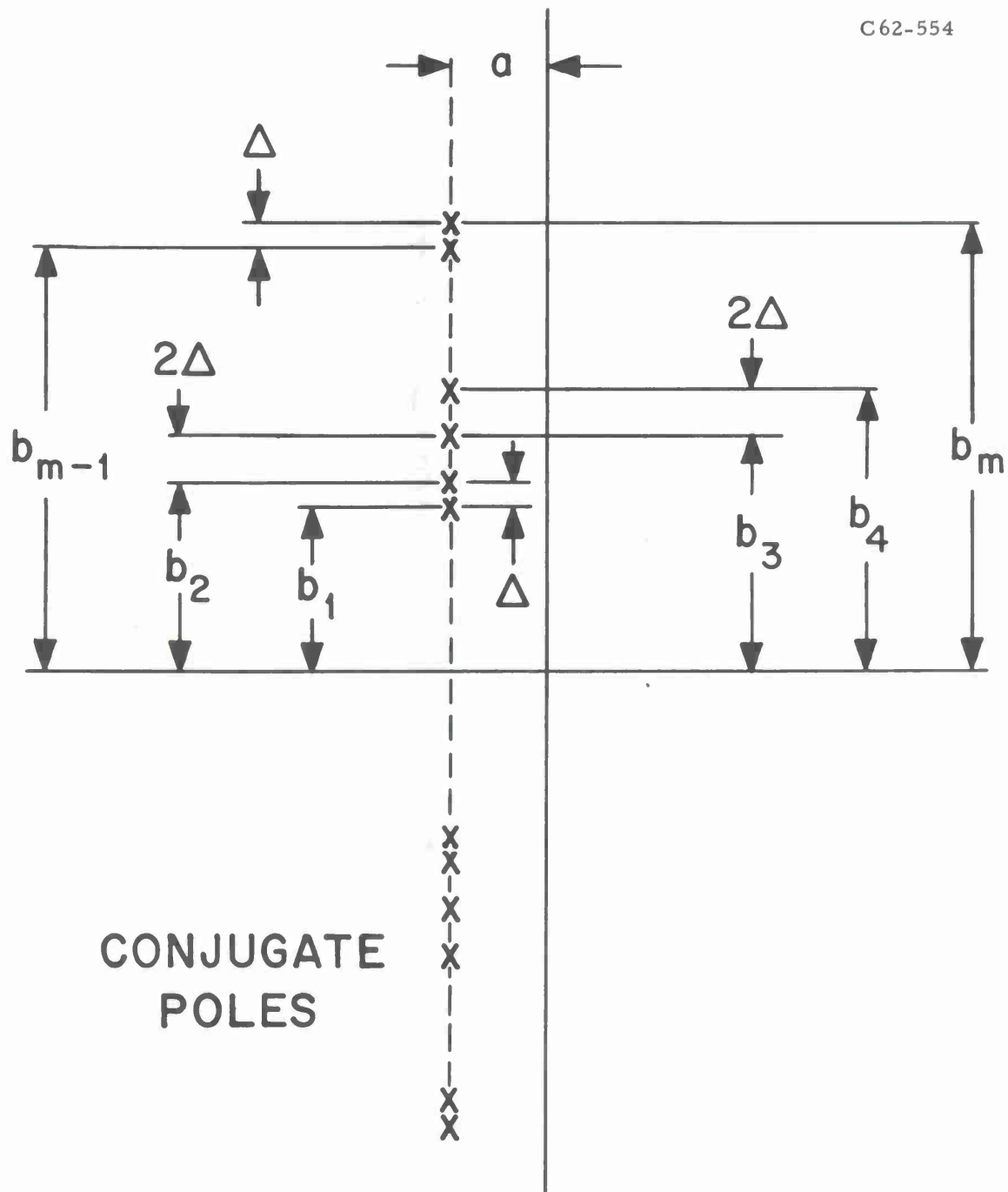
Fig. 7.    Pole positions for Lerner filter.

49
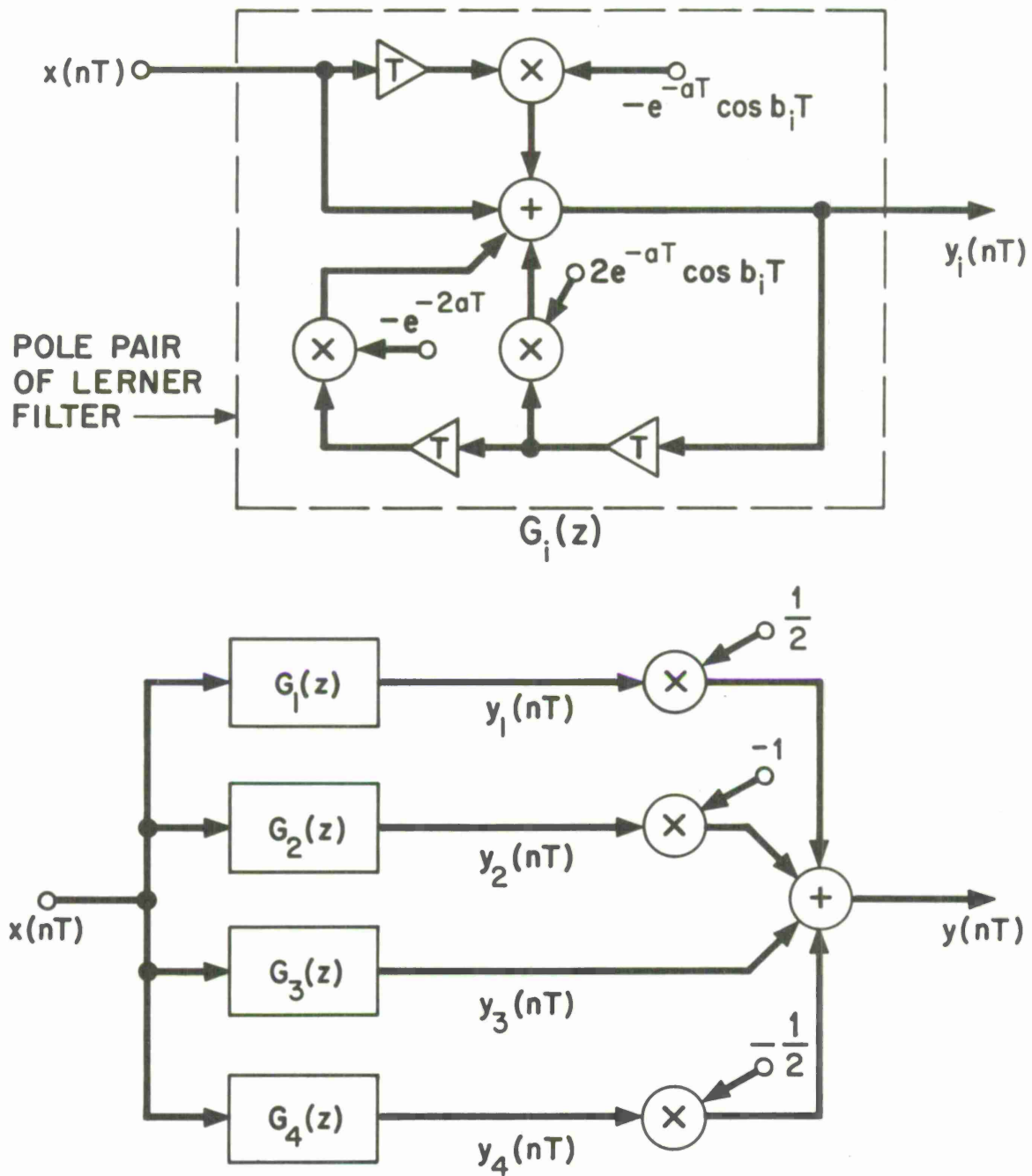
Fig. 8.   Configuration of $4^{th}$ order (8 pole) digital Lerner filter (dotted box shows configuration of pole pair $G_i(z)$).

51



$$\eta(\omega_c T) = e^{-\frac{1}{2}\omega_c T}\left(\cos\frac{\sqrt{3}}{2}\omega_c T + \frac{1}{\sqrt{3}}\sin\frac{\sqrt{3}}{2}\omega_c T\right)$$
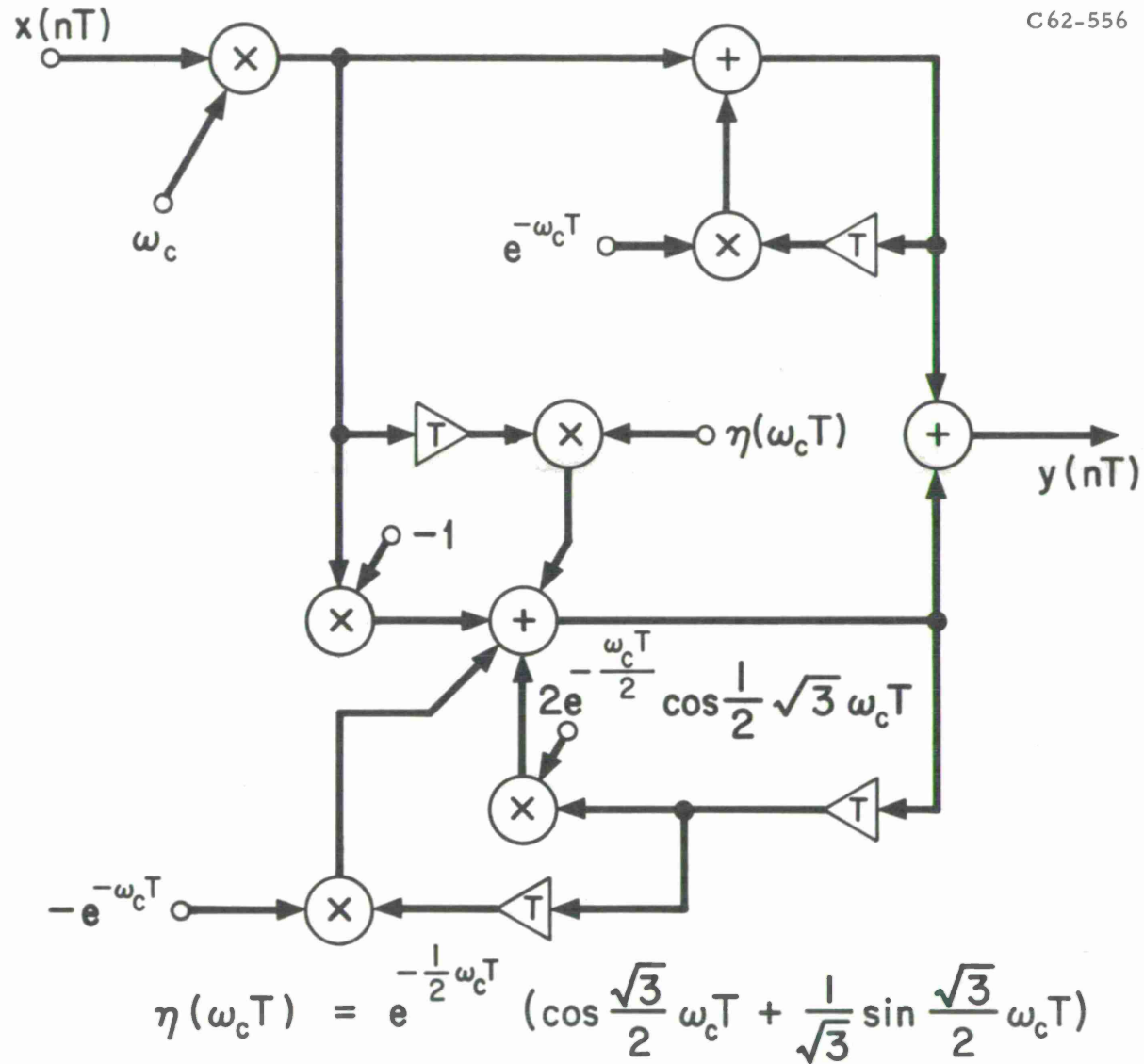
Fig. 9. Impulse invariant 3-pole Butterworth low pass filter.
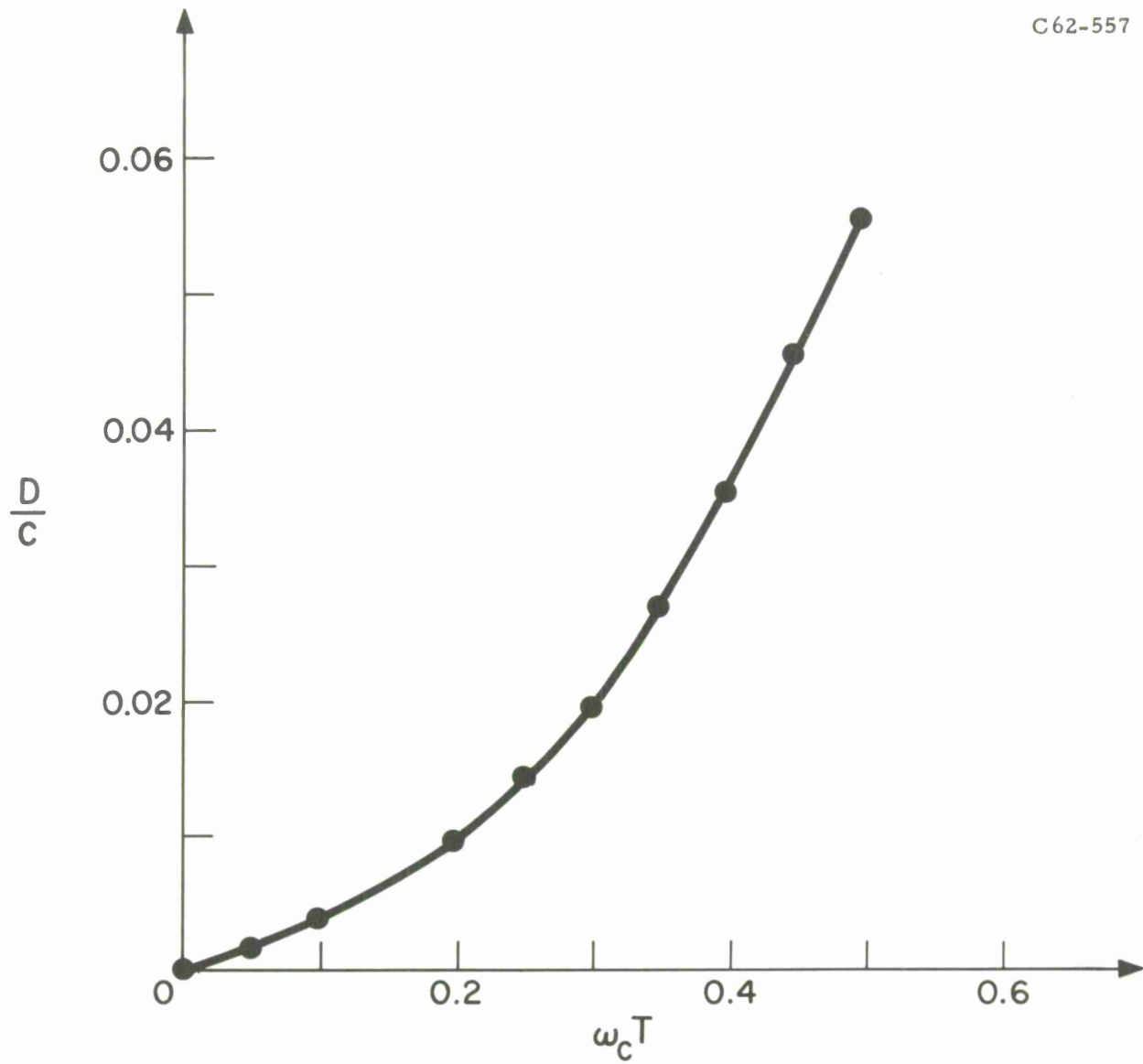
Fig. 10. Graph of $\dfrac{D}{C}$ showing position of extra zero introduced by impulse invariant design technique.
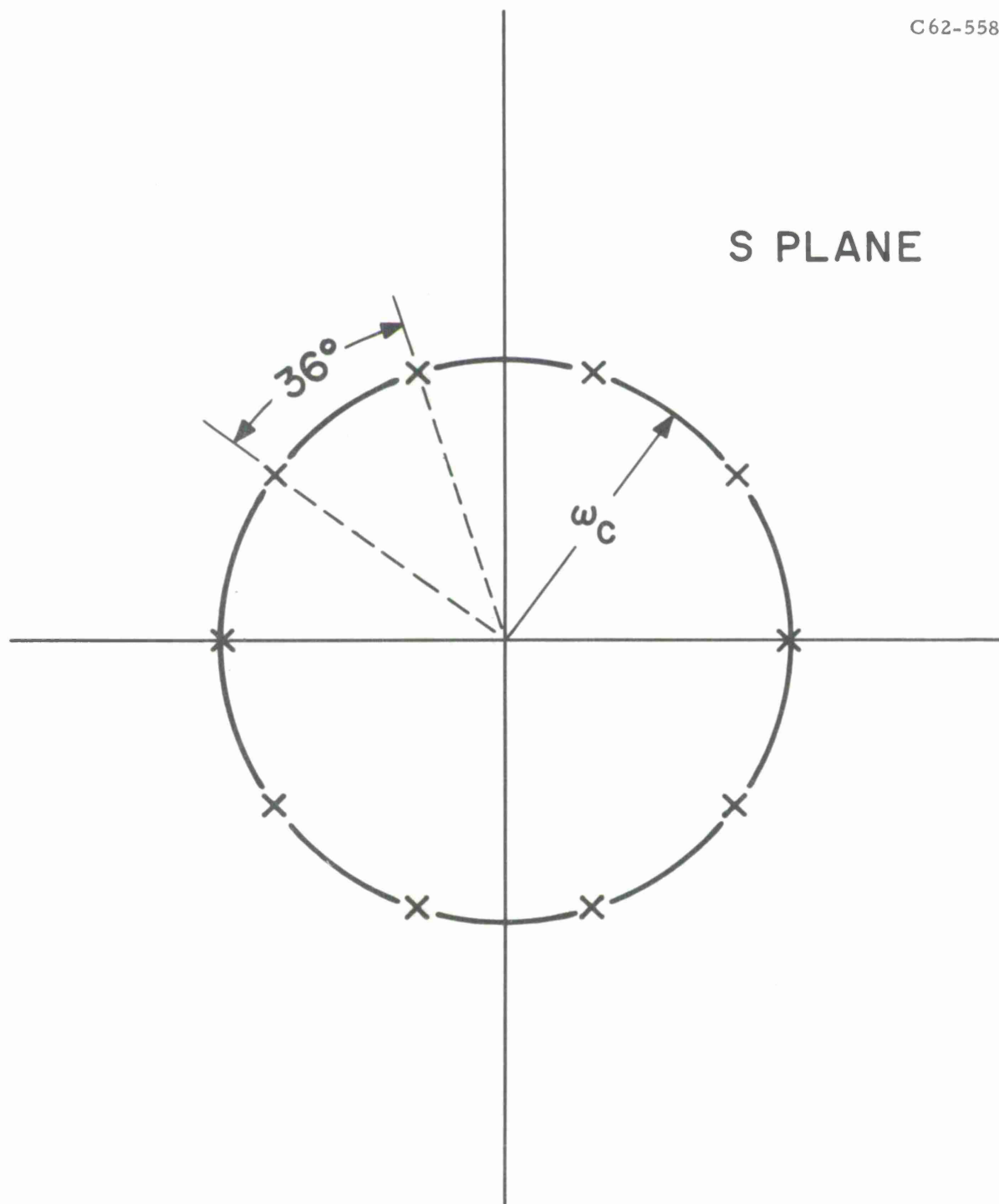
S PLANE

Fig. 11. Poles of Butterworth squared magnitude function, equation (44) for n = 5. Poles are equally spaced with angular separation 36°. The system function Y(s) is defined by the poles in left half plane.
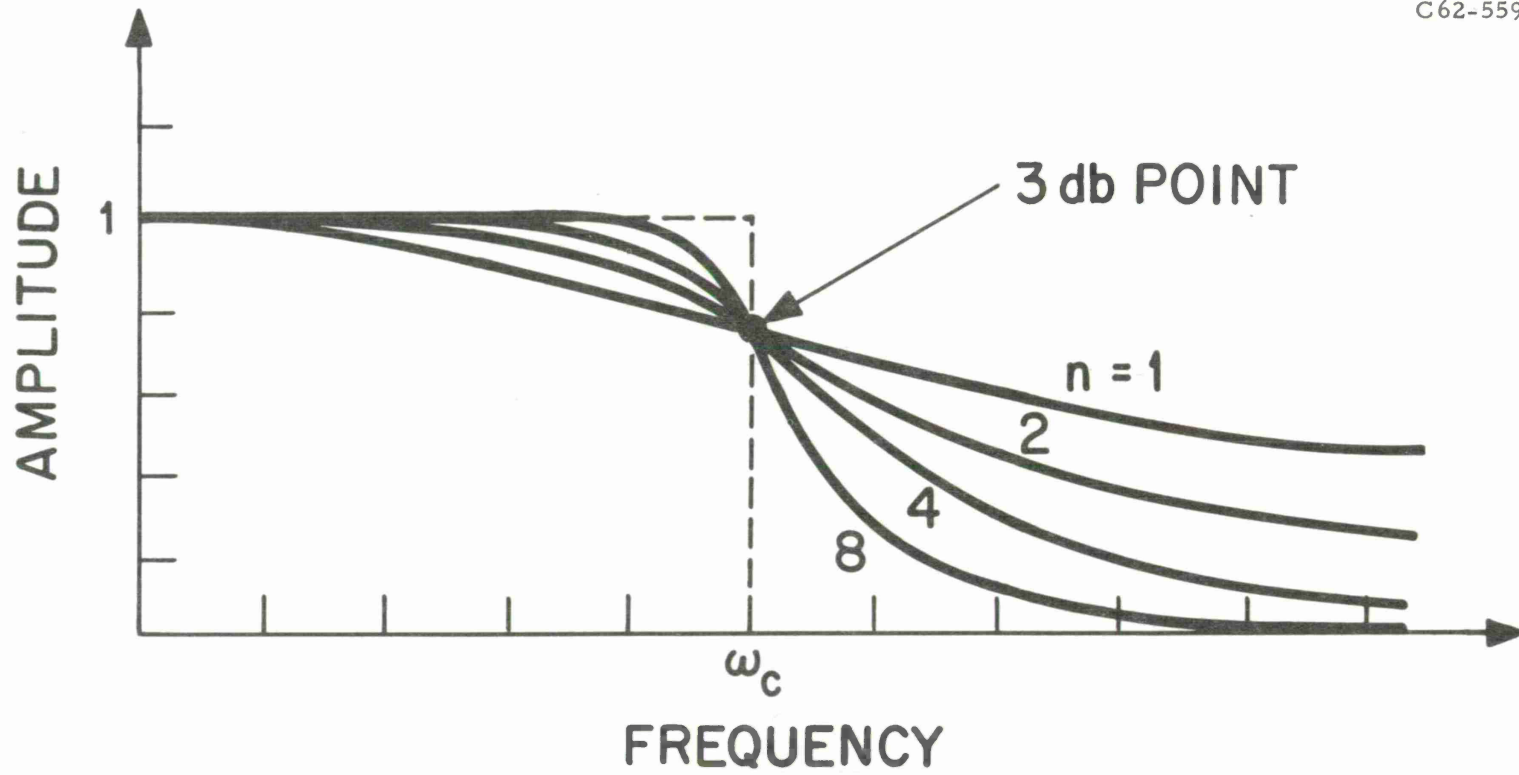
Fig. 12.   Magnitude vs frequency of Butterworth filters.
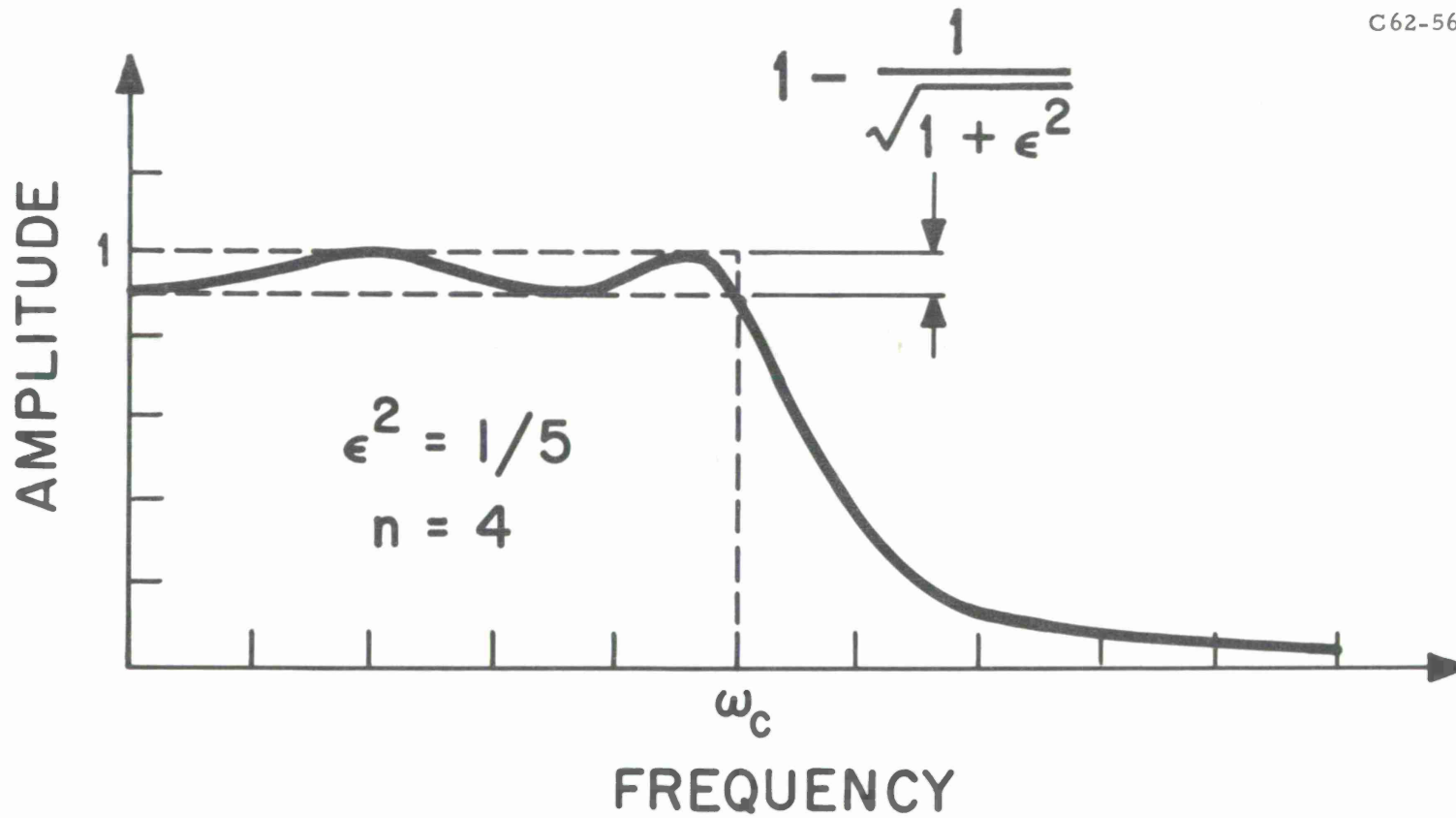
Fig. 13.   Magnitude vs frequency of 4$^{th}$ order Chebyshev low pass filter.

X CHEBYSHEV
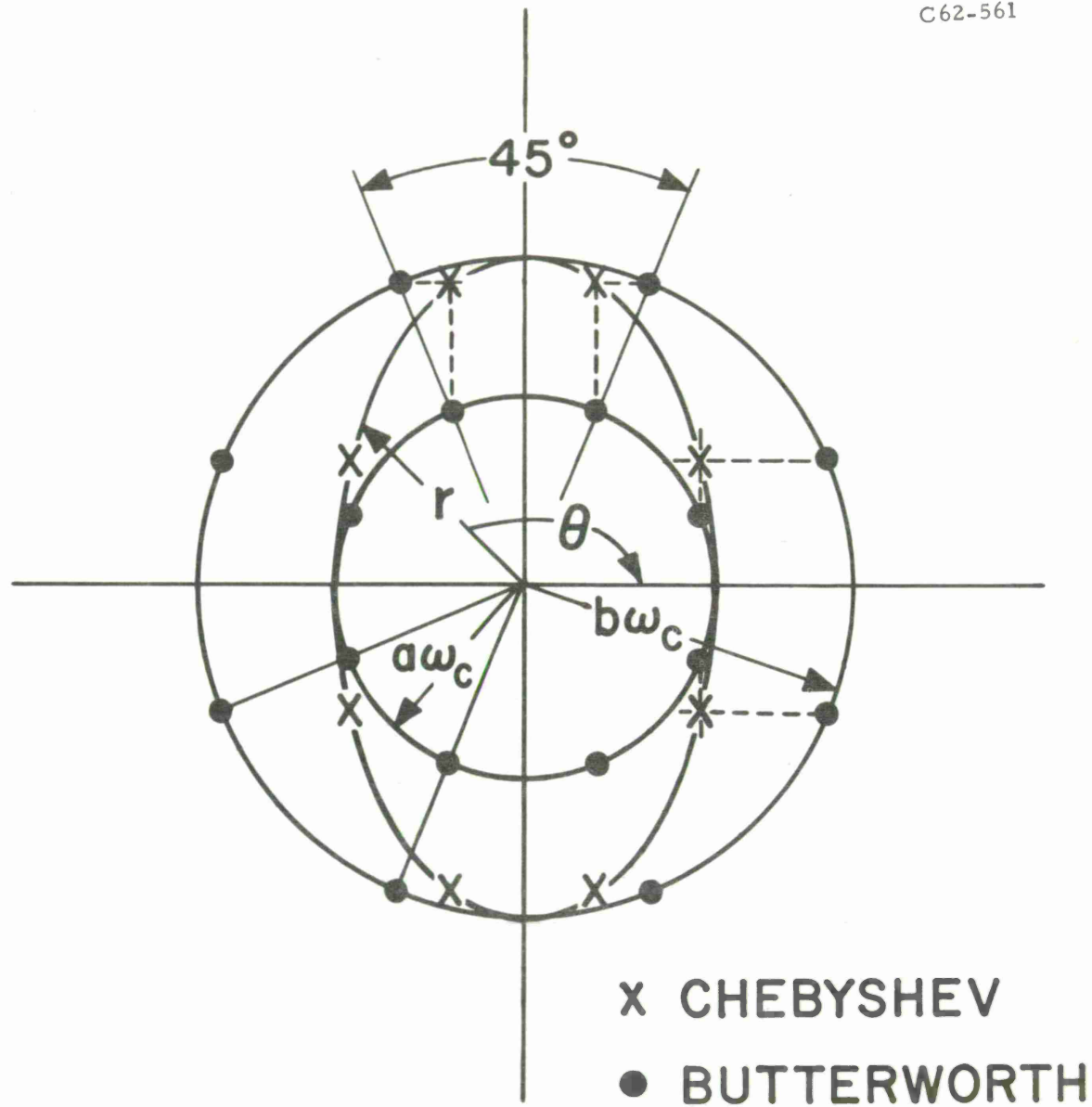
● BUTTERWORTH

Fig. 14. Poles of Chebyshev squared magnitude function for n = 4.
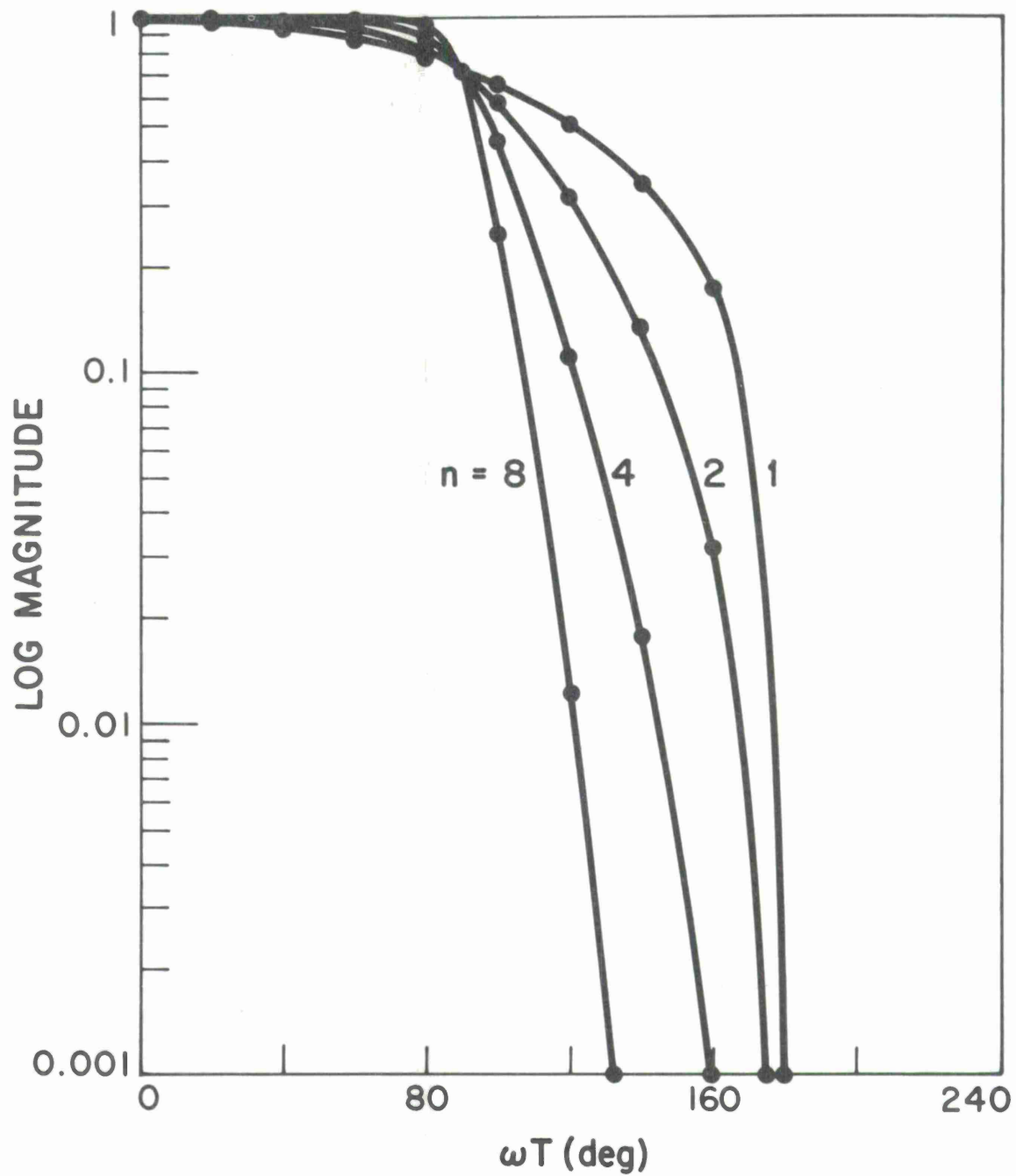
Fig. 15.   Magnitude vs frequency of frequency invariant digitized Butterworth filters.

$$\rho = \tan \frac{\omega_c T}{2}$$

$$\omega_c T = \frac{\pi}{4}, \quad \rho = 0.4142$$

$$\frac{1 + \rho^2}{1 - \rho^2}$$

C62-563

$z_2$

$z_1$

$z_3$

65.04°

32.64°

21.66°

51.26°

$z_4$

$z_5$

8th ORDER ZERO

$z_6$

$\frac{2\rho}{1 - \rho^2}$

$z_8$

$z_7$

1
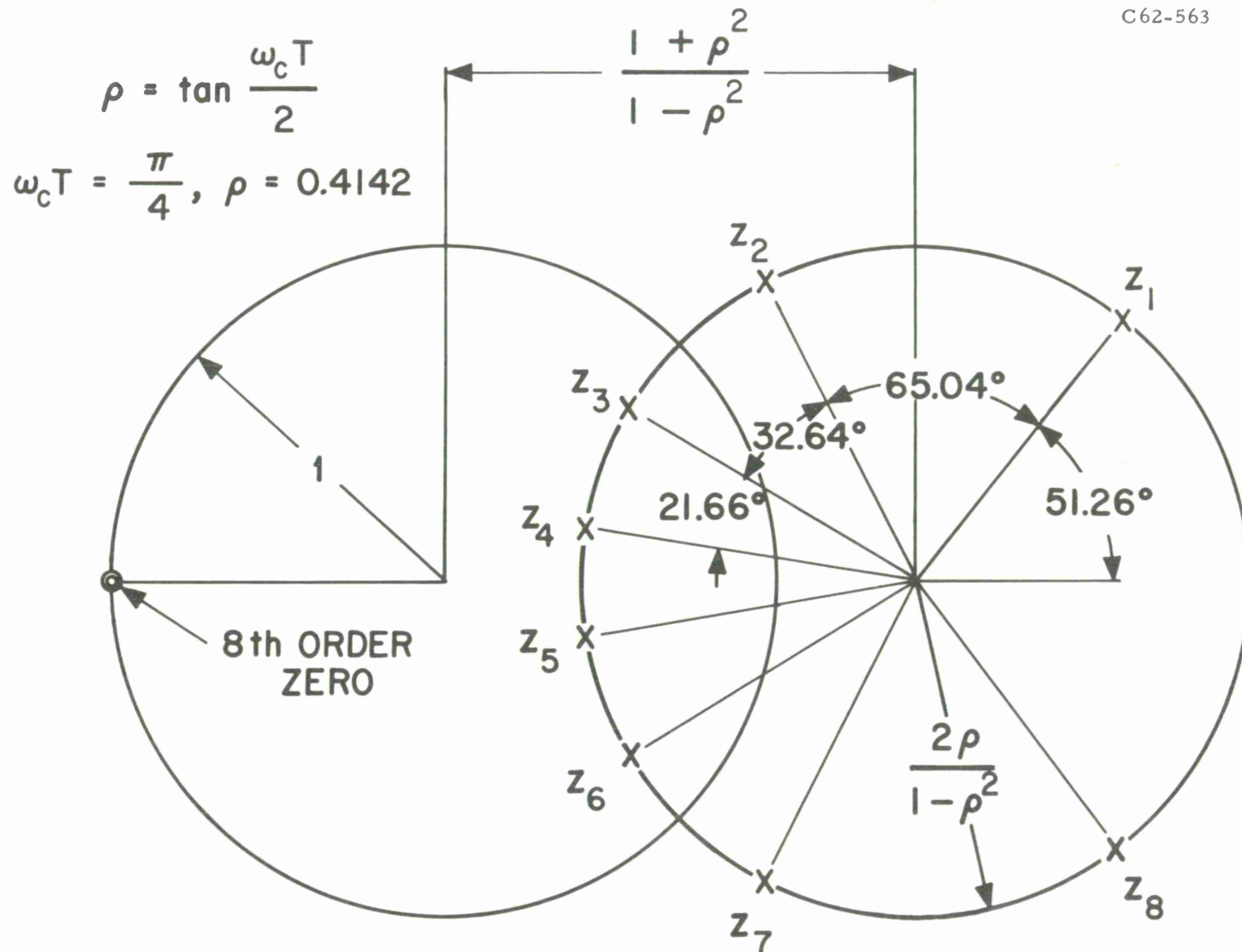
Fig. 16. Poles and zeros of squared magnitude function for example of section 2g.
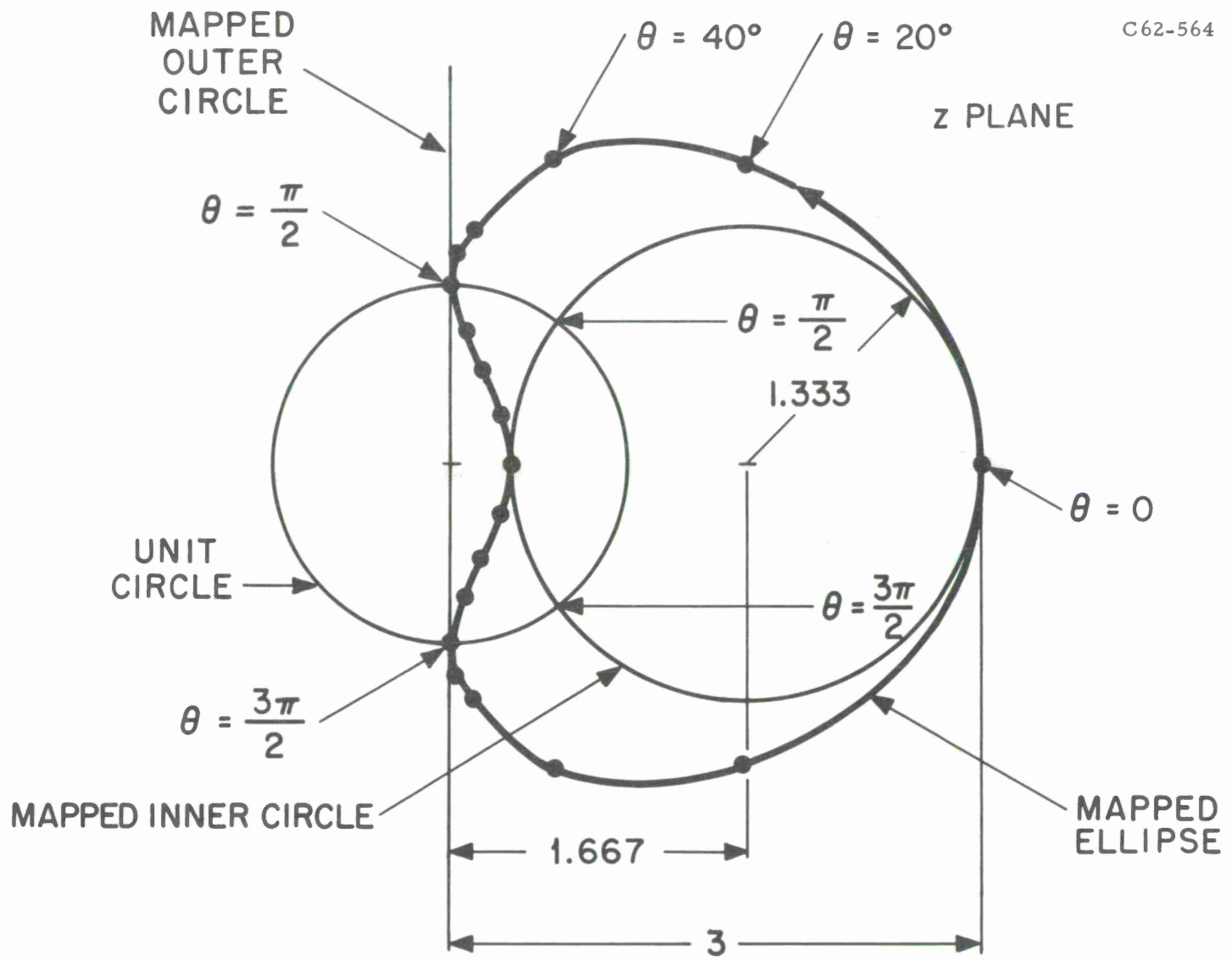
Fig. 17. Bilinear mapping of Chebyshev ellipse into z plane for

a $\tan \dfrac{\omega_c T}{2} = .5,$ b $\tan \dfrac{\omega_c T}{2} = 1.$ Points shown are mapped from 20 degree increments of $\theta$.

60
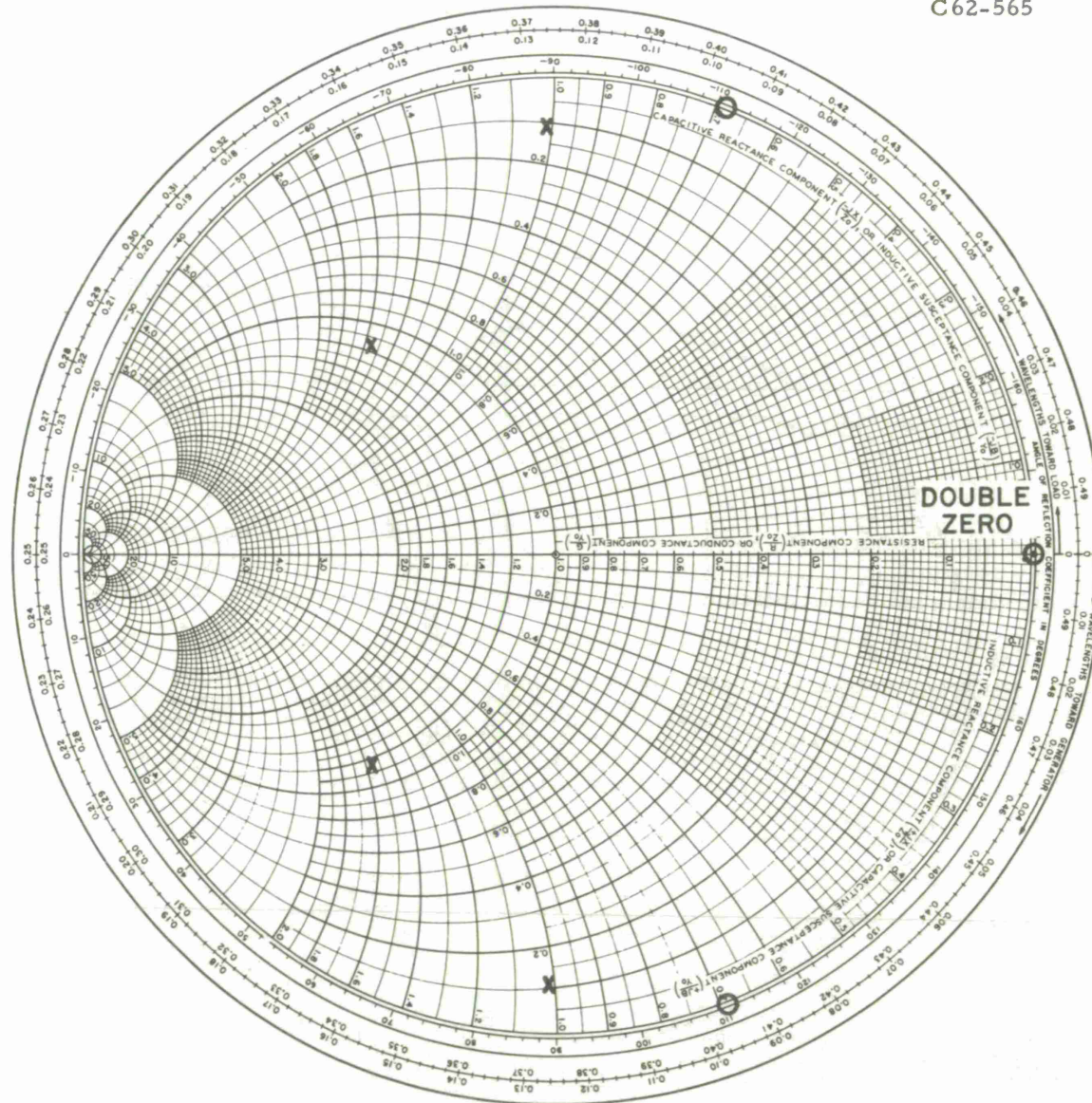


Fig. 18.   Poles and zeros of elliptic high pass filter, from Smith chart.
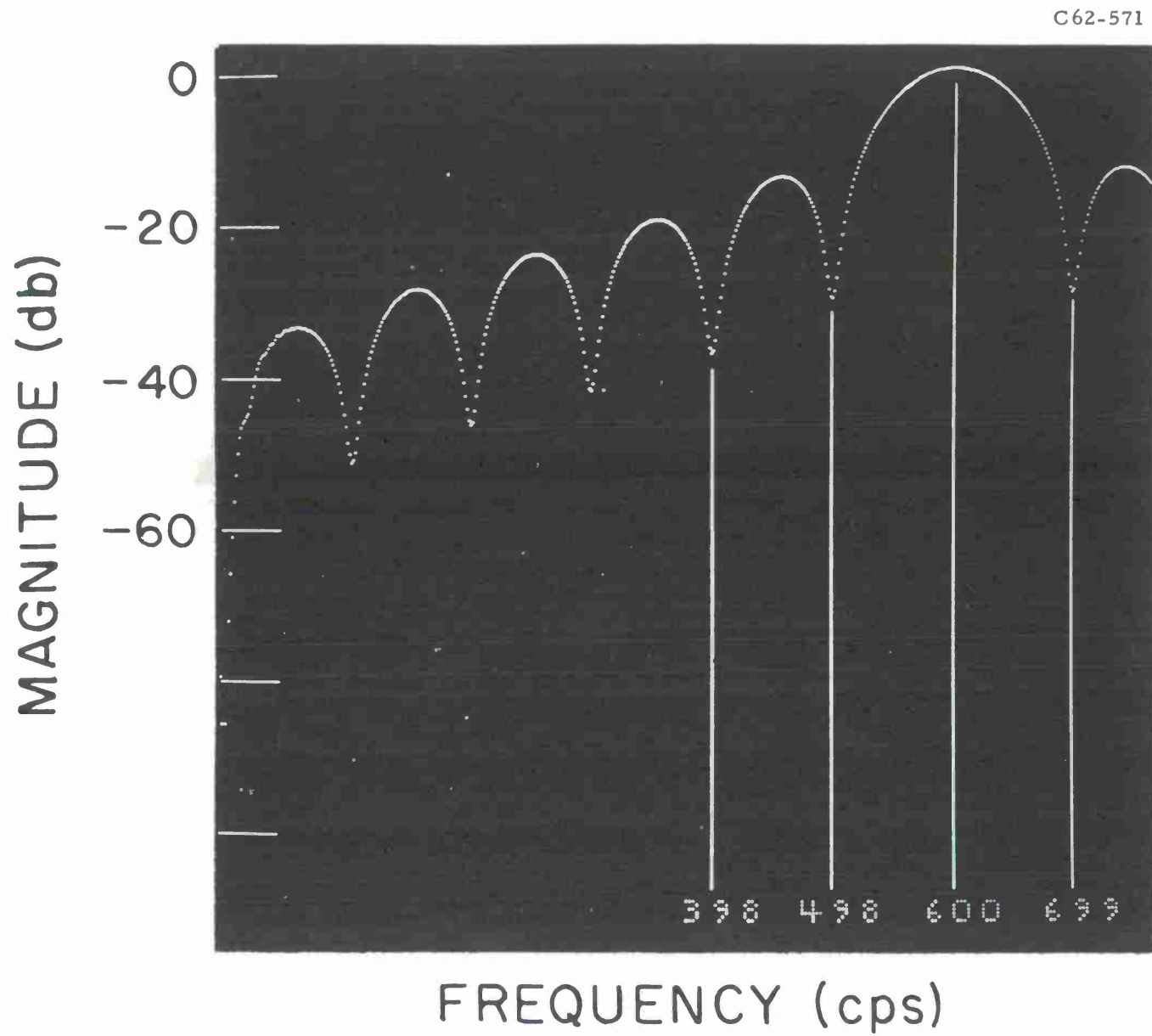
Fig. 19.   Response of elemental filter of equation (74).
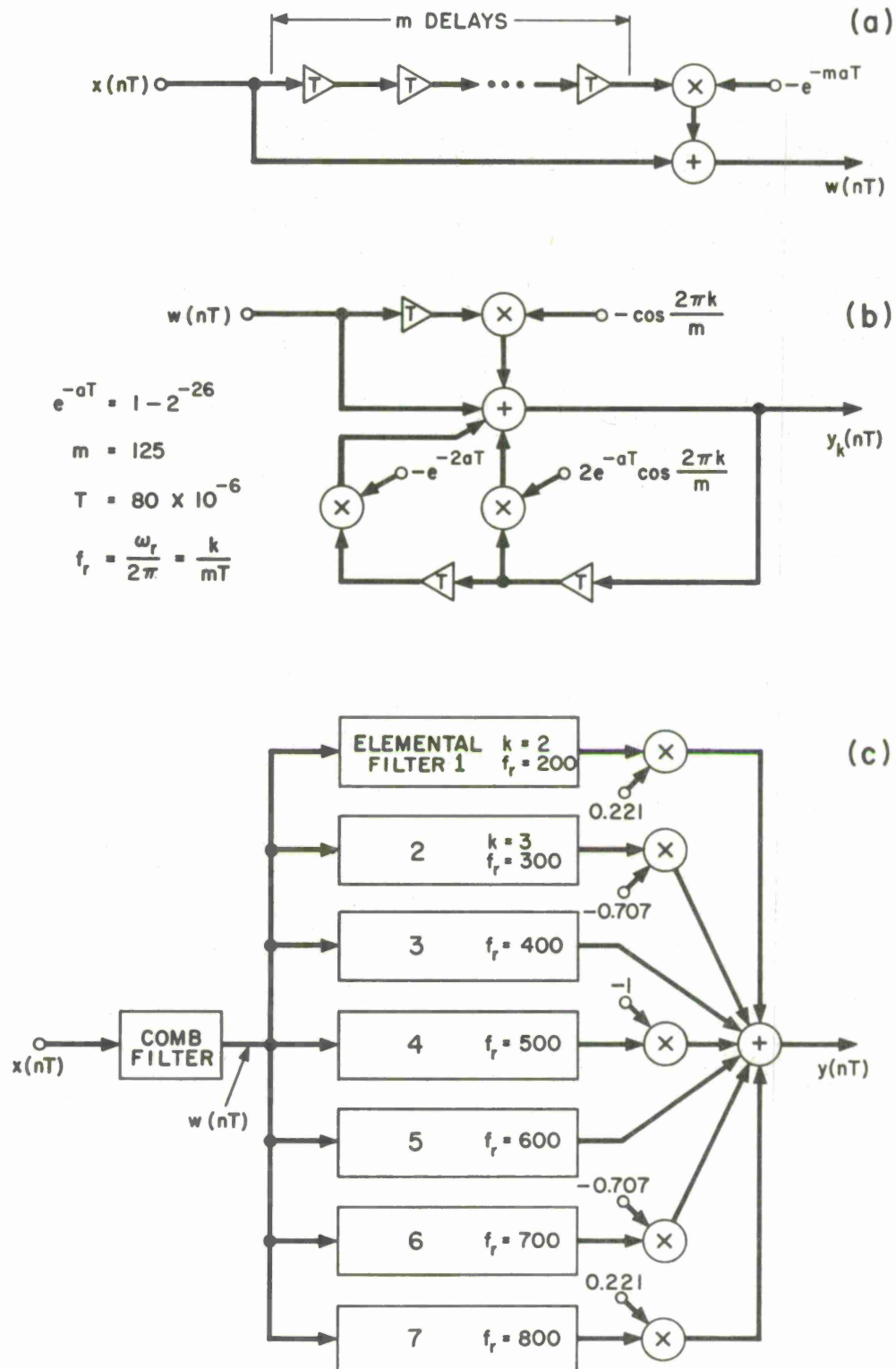
Fig. 20. Representation of frequency sampling filter with bandwidth from 300 cps to 700 cps. a) comb filter b) elemental filter c) complete filter.
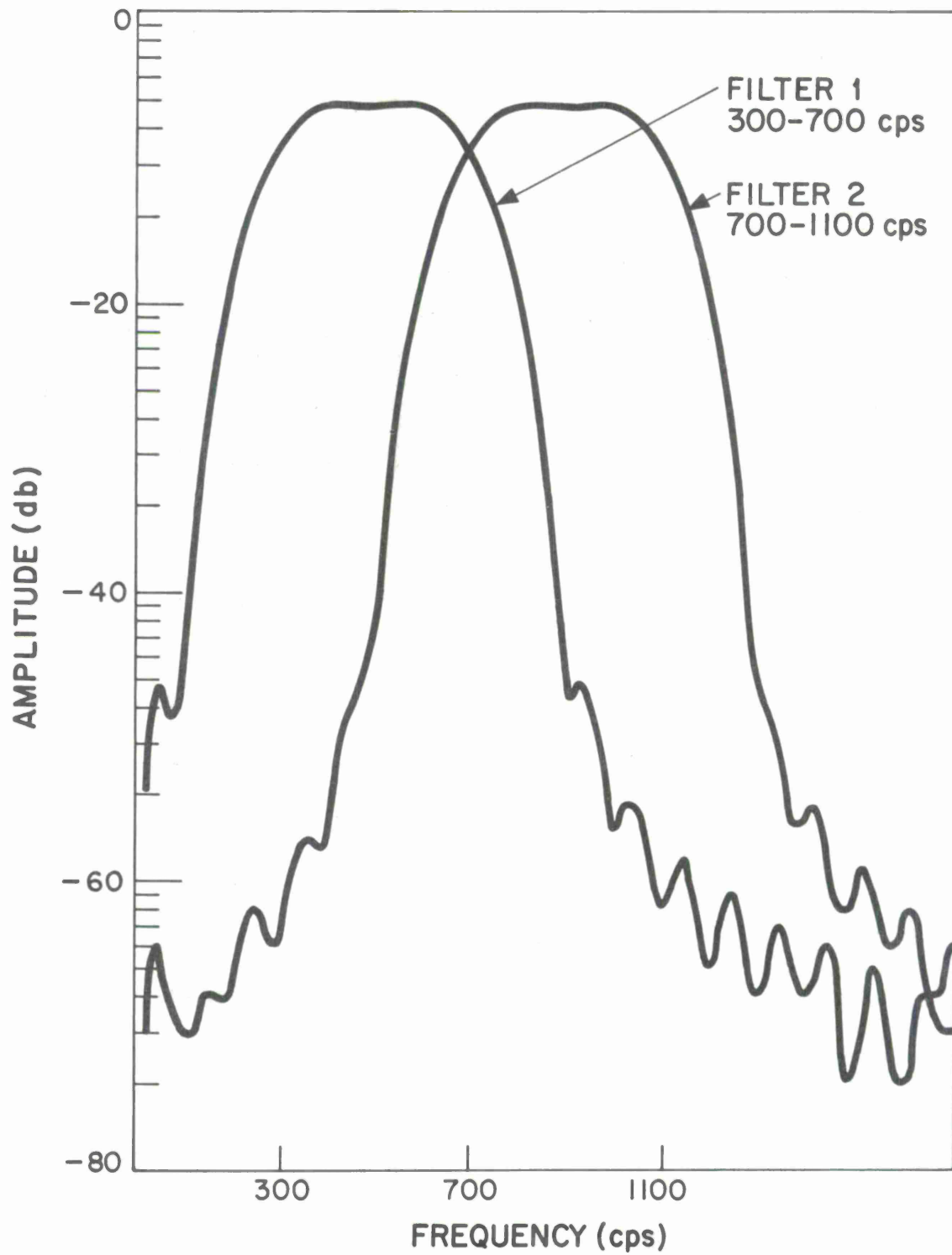
Fig. 21. Experimental amplitude vs frequency for contiguous band pass filters using frequency sampling technique.
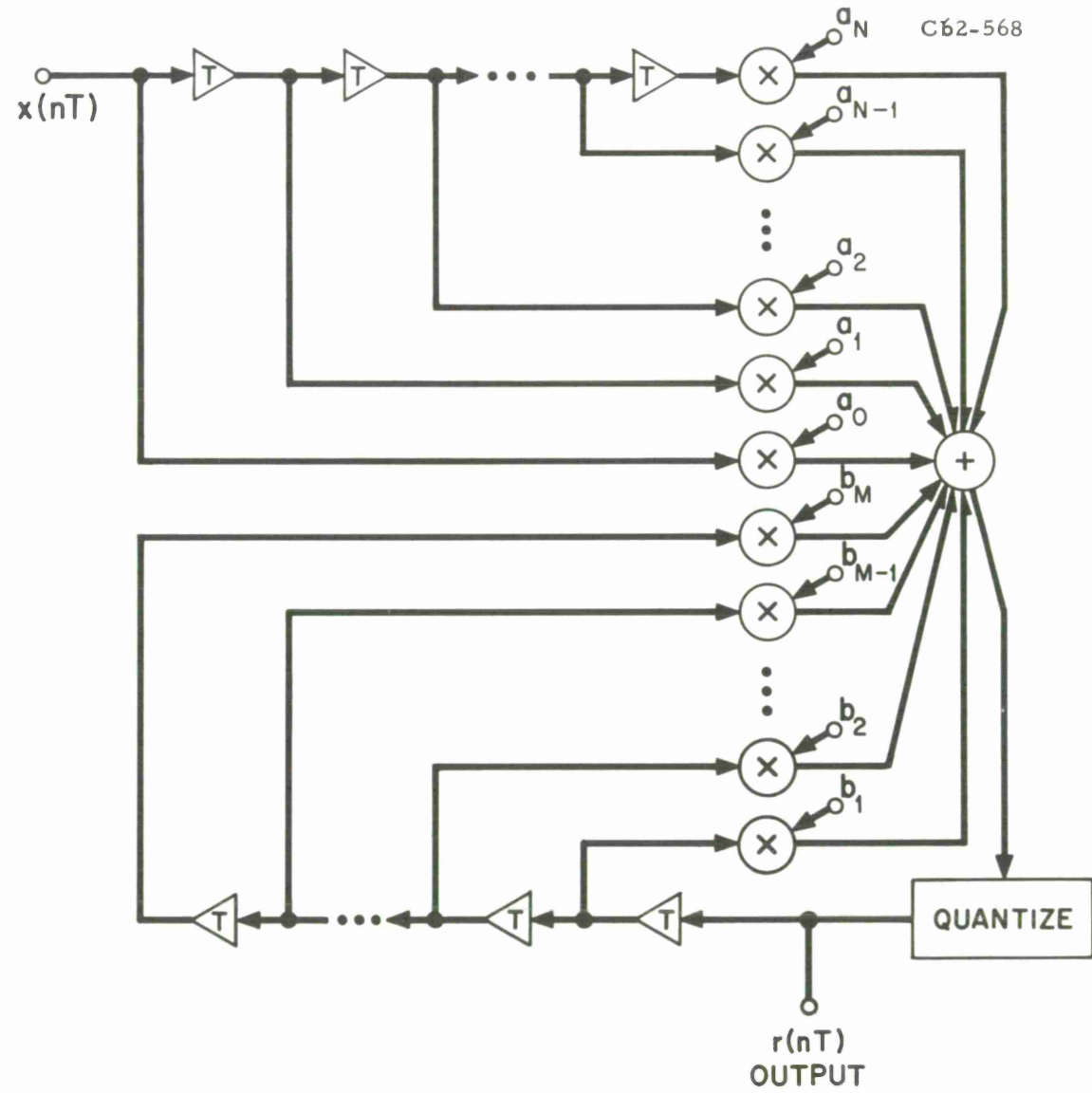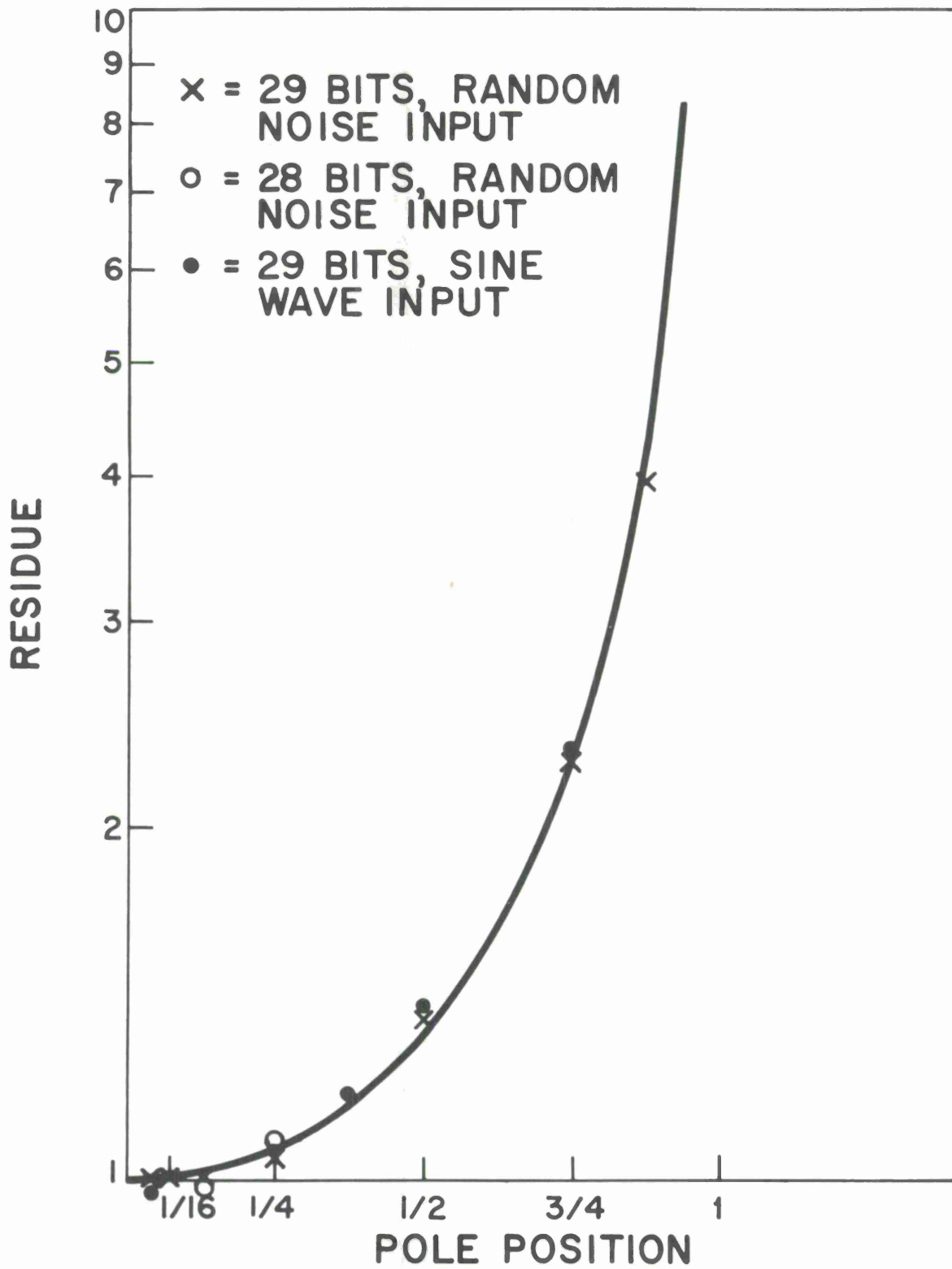
Fig. 22.   Digital filter with quantization error.

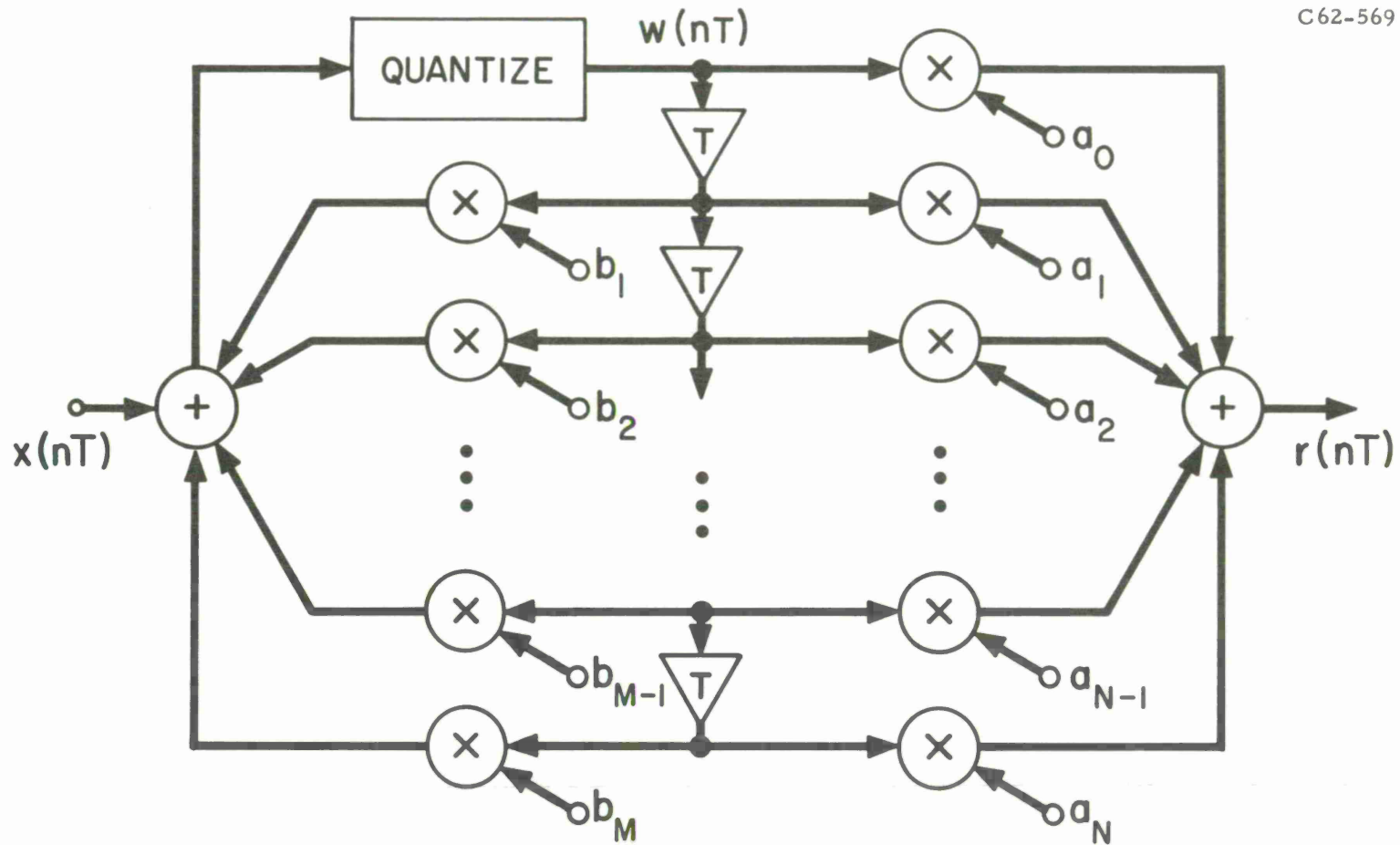Fig. 23.   Quantization noise for one pole filter.

Fig. 24. Canonical representation of digital filter with quantization (drawn for M = N).

# DISTRIBUTION LIST

Director's Office

W. H. Radford

Division 2

F. C. Frick

Group 23

J. I. Raffell
J. L. Mitchell
L. G. Roberts
W. R. Sutherland

Group 25

D. B. Yntema
J. W. Forgie
M. L. Groves
W. P. Harris
C. K. McElwain
O. G. Selfridge
A. N. Stowe
M. L. Wendell
R. A. Wiesen

Group 28

F. Schweppe
L. Gardner

Division 3

J. W. Meyer

Group 31

J. V. Evans
T. Hagfors

Group 32

E. A. Chatterton

Group 35

J. R. Bauer

Group 42

B. S. Goldstein

Group 46

R. M. Weigand

Group 47

D. L. Clark
R. P. Wishner

Division 6

G. P. Dinneen
W. E. Morrow

Group 61

L. J. Ricardi
R. N. Assaly
M. L. Burrows
R. K. Crane
M. E. Devane
B. F. LaPage
C. A. Lindberg
R. J. Peck
J. B. Rankin
M. L. Rosenthal
A. Sotiropoulos

Group 62

I. L. Lebow
F. E. Heart
P. R. Drouilhet
B. E. Nichols

R. Alter
J. H. Atchison
L. I. Blustein
G. Blustein
Y. Cho
J. W. Craig
W. R. Crowther
N. L. Daggett
J. D. Drinan
B. Gold
L. M. Goodman
D. H. Hamilton
J. N. Harris
H. H. Hoover
B. H. Hutchinson
K. L. Jordan
D. Karp
R. V. Locke

A. A. Mathiasen
P. G. McHugh
N. J. Morrisson
F. Nagy
C. W. Niessen
A. C. Parker
G. Ploussios
F. C. Popp
C. M. Rader
C. A. Reveal
S. B. Russell
P. D. Smith
I. Stiglitz
P. Stylos
R. Teoste
J. Tierney
D. K. Willim

## Group 63

H. Sherman
R. M. Lerner
D. C. MacLellan
P. Waldron
G. H. Ashley
R. S. Berg
A. Brag-Illa
H. C. Burrowes
R. W. Chick
N. B. Childs
M. C. Crocker
A. I. Grayzel

B. Howland
S. R. Hornig
J. Max
D. M. Mathanson
D. Parker
K. E. Shostack
D. M. Snider
D. Tang
N. R. Trudeau
W. R. Vecchia
E. A. Vrablik

## Group 64

E. J. Aho
W. D. Chapman
A. F. Dockrey
M. R. Goldberg
T. E. Gunnison
D. M. Hafford
L. F. Hallowell
D. A. Hunt

L. R. Isenberg
W. C. Provencher
R. J. Saliga
T. Sarantos
R. S. Tringale
D. C. Walden
S. J. White

P. E. Green
H. W. Briscoe
J. Capon
L. T. Fleck
P. L. Fleck
R. E. Gay
M. J. Flesher

E. Gehrels
R. J. Greenfield
E. J. Kelly
R. J. Kolker
R. T. Lacoss
R. M. Sheppard
C. A. Wagner
R. Walsh

## Group 65

H. Stahle
J. Delsie
R. Drapeau
J. Drobot
E. Edman
P. Gendron
A. Grennel
A. Kesselhuth
R. M. Kokoska
A. Lipofsky
Group 62 Files

R. MacKnight
M. MacAskill
A. Olson
A. Pearson
A. Peterson
J. Ritchie
S. Sawicki
J. Siemasko
C. Symonds
N. Vlahakis
R. Zemba

R. V. Wood
R. G. Enticknap
J. R. Brown
J. P. Densler
E. P. Edelson

L. W. Giusti
R. A. Guillette
E. W. Richards
C. B. Swanton
I. Wigdor

## Group 66

B. Reiffen
J. U. Beusch
T. J. Goblick
B. E. White

H. L. Yudkin
M. H. Simon

## Group 75

E. P. Gaudette

## Archives

68

AFCRL

Weiant Wathen-Dunn
Philip Leiberman
Caldwell P. Smith
William Strong

ESD

Herbert Rubenstein

MIT

Alvin D. Bedrosian
Amar G. Bose
Hugh Byers
James D. Bruce
Richard Clayton
Wilbur B. Davenport
Peter Elias
Robert M. Fano
Ercolino Ferretti
Anthony F. Gangi
Morris Halle
John M. Heinz
Marvin L. Minsky
Alan V. Openheim
Frank Press
Walter A. Rosenblith
William M. Siebert
Kenneth N. Stevens
Thomas S. Stockham
Hyoji Suzuki
M. Nafi Toksoz
Harry Van Trees
Thomas F. Weiss
John M. Wozencraft

The Mitre Corp.

Roger Manasse
Hawley K. Rising
Norman S. Zimbel

Advanced Research Projects Agency
Washington, D. C.

Robert A. Frosch
John DeNayer
Harry Sonnemann

Aerospace Corp.
P. O. Box 95085
Los Angeles, California

Harold F. Meyer

Air Force Avionics Laboratory
Wright-Patterson AFB, Ohio

Robert L. Remm

AFOAR (RROSG)
Tempo D
Washington, D. C.

Richard S. Bennett
Rowena Swanson

AFOSR (SRI)
Tempo D
Washington, D. C.

Harold Wooster

Air Force Technical Applications Center
Washington 25, D. C.

Carl F. Romney

Applied Psychology Research Unit
15 Chaucer Road
Cambridge, England

Donald Broadbent
Alan Carpenter
John Morton

Charles W. Adams Associates, Inc.
142 Great Road
Bedford, Massachusetts

Charles W. Adams

D. H. Baldwin Company
1801 Gilbert Avenue
Cincinnati, Ohio

D. W. Martin

Bell Telephone Labs
Murray Hill, New Jersey

Bruce P. Bogert
Edward E. David
Peter B. Denes
James L. Flanagan
Lawrence S. Frishkopf
Newman Guttman
James F. Kaiser
Lawrence G. Kersta
Max V. Mathews
John R. Pierce
H. I. Pollack
Manfred R. Schroeder
Dave Slepian

B. Bhimani
1838 Massachusetts Ave.
Lexington, Massachusetts

Bolt, Beranek & Newman, Inc.
50 Moulton Street
Cambridge, Massachusetts

Jordan J. Baruch
Leo L. Beranek
Michael H. L. Hecker
Thomas M. Marill
John A. Swets
Francis M. Wiener

70

Brigham Young University
Provo, Utah

Harvey Fletcher

British Embassy
3100 Mass. Ave. NW
Washington, D. C.

B. Moorehouse

California Institute of Technology
Seismological Laboratory
220 North San Rafael Avenue
Pasadena, California

Don L. Anderson
David Braverman
Frank Press
Steward W. Smith

Cambridge Language Research Unit
20 Millington Road
Cambridge, England

Margaret, Masterman

Central Research Laboratory
Hitachi, Ltd.
Kokobunji, Titatama
Tokyo, Japan

Tanetoshi Miura

Children's Hospital Medical Center
300 Longwood Avenue
Boston, Mass.

Allan C. Goodman

Clark School for the Deaf
46 Round Hill Road
Northampton, Mass.

Philip A. Bellefleur

Collins Radio Co.
Cedar Rapids, Iowa

Robert Craiglow

Columbia University
632 W. 125 Street
New York, N. Y.

Cyril M. Harris

Codex Corp.
222 Arsenal Street
Watertown, Mass.

Arthur Kohlenberg

Control Data Corp.
Minneapolis, Minnesota

Y. Chu

Communication Research Institute
3430 Main Highway
Miami, Florida

John C. Lilly

Defense Research Medical Labs.
Box 62, Postal St. "K"
Toronto, Ontario, Canada

Keith K. Neely

Data and Information Systems Div.
ITT Box 285
Paramus, New Jersey

Hyman Housman

Electronic Associates, Inc.
P. O. Box 582
Princeton, New Jersey

R. Vichnevotsky

Federal Aviation Agency
Washington 25, D.C.

Walter A. Spieth

Federal Scientific Corp.
615 W. 131 Street
New York, N.Y.

Mark R. Weiss

Harry R. Feldman Inc.
40 Accolon Way
Boston, Mass.

Harry R. Feldman

General Atronics Corp.
200 E. Mermaid Lane
Philadelphia, Pennsylvania

Harry Urkowitz

General Dynamics Corp.
1400 North Goodman Street
Rochester 9, New York

Robert A. Houde
Raymond Sanlirocco
Frank H. Slaymaker

The Geotechnical Corporation
3401 Shiloh Road
Garland, Texas

J. H. Hamilton

Gulton Industries
212 Durham Ave.
Meturchen, New Jersey

Donald Hertzfeld

Harvard University
Cambridge, Mass.

Norman Abramson
George von Bekesy
Roman Jakobson
George A. Miller
Anthony G. Oettinger
Wayne Slawson

Haskin Laboratory, Inc.
305 E. 43rd Street
New York, N. Y.

Franklin S. Cooper
Kathrine S. Harris

Hearing & Speech Center
Gallaudet Coll.
Washington, D.C.

James M. Pickett

Honeywell, Inc.
Research Dept., E.D.P. Div.
Waltham, Mass.

R. Lawrence

John Hopkins University
Baltimore, Maryland

David H. Friedman
Moise H. Goldstein
William H. Huggins

Houston Speech & Hearing Center
Texas Medical Center
1343 Moursund
Houston, Texas

Charles E. Speaks

72

Hughes Aircraft Co.
P.O. Box 90902
Los Angeles, California

L. ,C. Parode
Jerome E. Toffler

Huyck Corporation
777 Summer Street
Stamford, Connecticut

William O. Davis

IBM
Yorktown Heights
New York

James T. Cooley
Robert Garwin
J.C.R. Licklider

IBM
10301 West Lake Drive
Bethesda, Maryland

Robert G. Baron
W. Vanderkulk

IBM Research Lab
Monterey & Cottle Roads
San Jose, California

H. M. Truby
Robert M. Walker

Imperial College
London, England

Colin Cherry

Indiana University
Bloomington, Indiana

James P. Egan
Thomas A. Seblok

Information International Inc.
200 Sixth Street
Cambridge, Mass.

Edward Fredkin

Institute for Defense Analyses
400 Army Navy Drive
Arlington, Virginia

A. Rubenstein
J. P. Ruina

Institute of Geophys. and Planetary Phys
University of California
LaJolla, California

Freedman Gilbert
Richard A. Haubrich
Walter H. Munk

Institute fur Nachrichtentechnik
Breitschiedstrasse 2
Struttgart-N, Germany

Eberhard K. Zwicker

Jet Propulsion Laboratories
Pasadena, California

Gus Solomon

Joint Speech Research Unit
Eastcote Road
Ruislip
Middlesex, England

J. Swaffield

Laboratorium voor Medische Fysica
Bloemsingel 1
Groninger, Netherlands

Janwillem von den Berg

M. I. T. Center Development Office
292 Main Street
Cambridge, Mass.

Thomas T. Sandel

Melpar, Inc.
3000 Arlington Blvd.
Falls Church, Virginia

Joseph S. Campanella

National Bureau of Standards
Sound Section 6. 1
Washington, D. C.

E. L. R. Corliss

National Cash Register Co.
Dayton, Ohio

Klaus W. Otten

National Institutes of Health
Bethesda, Maryland

Norman F. Gerrie
James Bosma

National Security Agency
Ft. Meade, Maryland

Douglas L. Hogan
Mitford Mathews
Howard Rosenblum

Nazareth College
Box 129
Nazareth, Kentucky

Kay Lee Johnson

New York University
College of Engineering
New York, N. Y.

Louis Gerstman

Nippon Electric Co. , Ltd.
Communication Research Lab
1753 Shimonumabe
Kawasaki City, Japan

Kuniichi Nagata

Northeastern University
360 Huntington Ave.
Boston, Mass.

Sze-Hou Chang
Ladislaw, Dolansky

NASA Electronics Research Center
575 Technology Square
Cambridge, Mass.

Thomas E. Burke

NHK Giken
361 Kinutacho, Setagaya
Tokyo, Japan

Soichiro, Kuroki

Information Technol. Labs
12820 Coit Road
Dallas, Texas

Lawrence A. Yaggi

Office of Naval Research
Washington, D. C.

Gilbert C. Tolharst (Code 454)

Ohio State University
154 No. Oval Drive
Columbus, Ohio

John W. Black
Ilse Lehiste
William S. -Y Wang

Philco Scientific Lab
Philco Corp.
Blue Bell, Pennsylvania

Lawrence E. Cassel
Louis R. Focht
David M. Jurenko
Robert W. Steele
Charles F. Teacher

James M. Pickett
2561 Wateiside Drive N. W.
Washington, D. C.

Polytechnic Institute of Brooklyn
Dept. of Electrical Engineering
333 Jay Street
Brooklyn 1, New York

Ernest Angelo
Ludwig Braun
Sid Deutsch
Noel X. DeLessio
Donald F. Hunt.
Arthur Laemmel
Robert Lerner
Eli Mishkin
Athanaseus Papoulis
Jules Russell
George Schlesinger
Mischa Schwartz

Psycholinguistics Laboratory
154 North Oval Drive
Columbus, Ohio

Henry M. Noser

Purdue University
Dept. of Electrical Engineering
West Lafayette, Indiana

Charles V. Anderson
Arthur S. House
George W. Hughes

Thomas Ramo-Wooldridge Inc.
8433 Fallbrook Ave.
Canoga Park, California

Paul L. Garvin

Rand Corporation
1700 Main Street
Santa Monica, California

Willis H. Ware

Raytheon Co.
20 Seyon Street
Waltham, Mass.

Laurence Batchelder

Radio Corp. of America Labs.
Camden, New Jersey

Willard F. Meeker

Radio Corp. of America
Princeton, New Jersey

Harry F. Olson

Rice University
Houston, Texas

Paul Pfeiffer

Rome Air Development Center
Griffiss AFB
New York

Frederick T. Becker
Raymond J. Christman

Signals Research and Dev. Establishment
Christchurch (Hants.), England

Leslie G. Stead

Speech Transmission Laboratory
Kungl Teknika Hogskolan
Stockholm 70, Sweden

C. Gunnar M. Fant

Standard Telecommunication Laboratories
London Road
Harlow, England

David R. Hill

Stanford Research Institute
333 Ravenswood Ave.
Menlo Park, California

Frank R. Clarke
Karl D. Kryter
William A. Runge
Stephen E. Stuntz

Stanford University
Palo Alto, California

Dorothy Huntington
Thomas Kailath
Emanuel Parzen
D. R. Reddy
Earl D. Schubert

Sperry Rand Research Center
North Road
Sudbury, Mass.

Robert Price

State University of New York
Dept. of Psychology
Cortland, New York

John F. Corso

Subcommittee on Noise Research Center
327 S. Alvarado Street
Los Angeles, California

Aram Glorig

Sylvania Electronics Products, Inc.
Applied Research Lab
Waltham, Mass.

Benjamin M. Eisenstadt
Harold J. Manley
James E. Storer

Syracuse University
821 University Ave.
Syracuse 10, New York

Josef J. Zwislocki

Tata Institute of Fundamental Research
Computer Section
Colaba
Bombay 5, India

P. V. S. Rao

Technische Universitat
1 Berlin 12, Germany

Fritz Winckel

Texas Instruments, Inc.
Dallas, Texas

Milo M. Backus
Richard Baldwin
John Burg
Renner B. Hofmann
Harry Lake
Stanley J. Laster
William Schneider
Larry Strickland
D. R. Ziemer

Ronald Tikofsky
1111 E. Catherine Street
Ann Arbor, Michigan

USAEL
Ft. Monmouth, New Jersey

Joseph DeClerk
Douglas L. Phyfe
Martin Weinstock

U.S. Army Signal Research & Dev. Lab
Ft. Monmouth, New Jersey

Bernard Goldberg
Arthur H. Russ

U.S. Arms Control & Disarmament Agency
Dept. of State
Washington 25, D.C.

R. S. Gellner

U.S. Naval Electronics Lab
San Diego, California

Robert S. Gales
Ray G. Klumpp
John C. Webster

U.S. Naval Medical Research Laboratory
Auditory Research Branch
Submarine Base
Groton, Connecticut

Donald J. Harris
Russell L. Sargeant

U.S. Naval Research Laboratory
Code 5412
Washington, D.C.

Wayne M. Jewett
Robert M. Mason (Code 4558)

United Electro Dynamics, Inc.
300 North Washington Street
Alexandria, Virginia

William C. Dean
Edward A. Flinn
Paul Broome

University of California
Berkeley 4, California

Harry D. Huskey
David J. Sakrison
Lofti A. Zadeh
Moshe Zakai

University of California
Dept. of Psychology
Davis, California

Jarvis Bastian

University of California
Los Angeles, California

Edward C. Carterette
Solomon Golomb
Mieko S. Han
Peter Ladefoged
Hans von Leden
Irving Reed

University College
Dept. of Phonetics
Gower Street
London, W.C.1, England

Dennis B. Fry

University of Colorado
Boulder, Colorado

Hans Wangler

University of Connecticut
Dept. of Psychology
Storrs, Connecticut

Alvin M. Liberman

University of California
Santa Barbara, California

Pierre Delattre

University of Edinburgh
Dept. of Phonetics
Minto House, Chambers St.
Edinburgh, Scotland

David Abercrombie
Walter Lawrence

University of Electro-Communications
14 Kojima-cho, Chofu
Tokyo, Japan

Osamu Fujimura

University of Hawaii

W. W. Peterson

University of Kyoto
Dept. of Oto-Rhino-Laryngology
Kawaramachi, Shoroin, Sakyoku
Kyoto City, Japan

Mitsukaru Gato

University Lektor Eli Fischer-Jorgensen
Kongestien 45
Virum, Denmark

Eli Fischer-Jorgensen

University of Miami
Virginia Key
Miami, Florida

John C. Steinburg

University of Michigan
P.O. Box 618
Ann Arbor, Michigan

T. W. Caless
Hugh K. Dunn
Gordon E. Peterson
Irwin Pollack
William L. Roog
Wilson P. Tanner

University of Minnesota
Box 461 Mayo
Minneapolis, Minnesota

W. Dixon Ward

University of Pennsylvania
Philadelphia, Pennsylvania

Belmont Favley
David M. Green
Andre Malecot
Harris B. Savin

78

University of Tokyo
Dept. of Electronic Engineering
Bunkyo-ku
Tokyo, Japan

Hiroya Fujisaki

University of Toronto
Dept. of Psychology
Toronto, Canada

Douglas C. Creelman

Utah State University
Logan, Utah

Samuel G. Fletcher

Washington University
Computer Research Lab
700 South Euclid Avenue
St. Louis, Missouri

Wesley Clark
Charles Molnar
William Papian

Wayne State University
Speech and Hearing Clinic
Detroit, Michigan

George A. Kapp

Weston Observatory
319 Concord Road
Weston, Mass.

Father David M. Clark

# DOCUMENT CONTROL DATA – R&D

*(Security classification of title, body of abstract and indexing annotation must be entered when the overall report is classified)*

| 1. ORIGINATING ACTIVITY *(Corporate author)* | 2a. REPORT SECURITY CLASSIFICATION |
|---|---|
| Lincoln Laboratory, M. I. T. | Unclassified |
| | 2b. GROUP<br>None |

**3. REPORT TITLE**

Digital Filter Design Techniques

**4. DESCRIPTIVE NOTES** *(Type of report and inclusive dates)*
Technical Note

**5. AUTHOR(S)** *(Last name, first name, initial)*

Rader, Charles M.
Gold, Bernard

| 6. REPORT DATE | 7a. TOTAL NO. OF PAGES | 7b. NO. OF REFS |
|---|---|---|
| 23 December 1965 | 84 | 18 |

| 8a. CONTRACT OR GRANT NO. | 9a. ORIGINATOR'S REPORT NUMBER(S) |
|---|---|
| AF 19 (628)-5167 | Technical Note 1965-63 |
| b. PROJECT NO.<br>649L | |
| c. | 9b. OTHER REPORT NO(S) *(Any other numbers that may be assigned this report)* |
| d. | ESD-TDR-65-593 |

**10. AVAILABILITY/LIMITATION NOTICES**

None

| 11. SUPPLEMENTARY NOTES | 12. SPONSORING MILITARY ACTIVITY |
|---|---|
| None | Air Force Systems Command, USAF |

**13. ABSTRACT**

Digital filtering is the process of spectrum shaping using digital components as the basic elements. Increasing speed and decreasing size and cost of digital components make it likely that digital filtering, already used extensively in the computer simulation of analog filters, will perform, in real-time devices, the functions which are now performed almost exclusively by analog components. In this paper, using the z-transform calculus, several digital filter design techniques are reviewed, and new ones are presented. One technique can be used to design a digital filter whose impulse response is like that of a given analog filter; another technique is suitable for the design of a digital filter meeting frequency response criteria. A third technique yields digital filters with linear phase, specified frequency response, and controlled impulse duration. The effect of digital arithmetic on the behavior of digital filters is also considered.

**14. KEY WORDS**

| | | |
|---|---|---|
| digital filters | bandpass filters | network theory |
| design | circuits and components | z-transform theory |
| digital systems | difference equations | speech compression |